

# **MODELLING AND SIMULATION OF A TCSC COMPENSATED POWER SYSTEM**

**A DISSERTATION**

*Submitted in partial fulfillment of the  
requirements for the award of the degree*

*of*

**MASTER OF TECHNOLOGY**

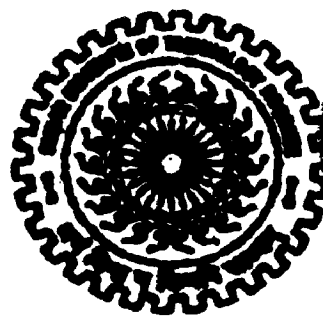
*in*

**ELECTRICAL ENGINEERING**

*(With Specialization in System Engineering & Operations Research)*

**By**

**LALATENDU GURU**



**DEPARTMENT OF ELECTRICAL ENGINEERING  
INDIAN INSTITUTE OF TECHNOLOGY ROORKEE  
ROORKEE -247 667 (INDIA)  
JUNE, 2006**

## CANDIDATE'S DECLARATION

---

I hereby declare that the work, which is being presented in this dissertation entitled "**Modelling and Simulation of a TCSC Compensated Power System**" in the partial fulfillment of the requirement for the award of the degree of **Master of Technology in Electrical Engineering** with specialization in **System Engineering and Operation Research**, submitted in the **Department of Electrical Engineering, Indian Institute of Technology Roorkee, Roorkee**, is an authentic record of my own work carried out during **July 2005 to June 2006** under the supervision of **Prof. H. O. Gupta**, Professor and **Dr. G. N. Pillai**, Assistant Professor, Department of Electrical Engineering, IIT Roorkee.

I have not submitted the matter embodied in this dissertation for award of any other degree.

**Date:**

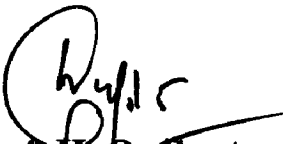
**Place: Roorkee**

*Lalatu Guru*  
(Lalatu Guru)

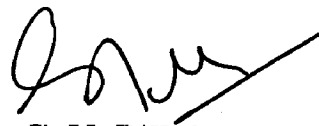
---

## CERTIFICATE

This is to certify that the above statement made by the candidate is true to the best of my knowledge and belief.



**Prof. H. O. Gupta**  
Professor,  
Department of Electrical Engineering,  
Indian Institute of Technology Roorkee.  
Roorkee – 247667.



**Dr. G. N. Pillai**  
Assistant Professor,  
Department of Electrical Engineering,  
Indian Institute of Technology Roorkee.  
Roorkee – 247667.

## ACKNOWLEDGEMENTS

---

I wish to express my deep sense of indebtedness and sincerest gratitude to **Prof. H. O. Gupta**, Professor and **Dr. G. N. Pillai**, Assistant Professor, Department of Electrical Engineering, Indian Institute of Technology Roorkee, Roorkee, for their invaluable guidance, cogent discussion and constructive criticism throughout this dissertation. They displayed unique tolerance and understanding at every step of progress and encouraged me incessantly. I deem it privilege to have carried out my Dissertation work under their able guidance.

I express my appreciation and thanks to Mr.Sidharth Panda, Mr.Deepak Nagariya and Mr.Bhawesh, Research Scholar, Dept.of Electrical Engineering, for free exchange of ideas and discussions which proved helpful.

Special thanks due to Varaprasad, Dilip, Vijayprasad, who have graciously applied themselves to the task of helping me with moral support and valuable suggestions, during my stay in IIT Roorkee. I am also thankful to Mr.Utpal Kumar Nath for the proof reading.

I wish to acknowledge the affection and moral support of my family member, for being so understanding and helpful during this period.

Finally, I am thankful and grateful to God the Almighty for ushering his blessings on all of us.

**(Lalatendu Guru)**

## ABSTRACT

---

The objective of this dissertation report is to model and analyze small signal torsional oscillations such as Sub synchronous resonance (SSR) characteristic of a Thyristor controlled series capacitor (TCSC) compensated power system. The power system used in this study is the IEEE first benchmark model for SSR analysis. A new model of TCSC is used in the study which includes the complete model of the controller. The turbine shaft, the generator and the TCSC are modeled using linearized equations. TCSC is regulated by a simple PI controller and a phase locked loop (PLL).

The torsional characteristics are studied through eigenvalue analysis and the results are validated through PSCAD/EMTDC simulation studies.

---

Acknowledgement	iii
Abstract	iv
List of figures	vii
Chapter-1 Introduction	1
1.1 Introduction	1
1.2 Subsynchronous resonance (SSR)	2
1.2.1 Induction Generator Effect	2
1.2.2 Torsional Interaction Effect	3
1.2.3 Transient Torque Effect	3
1.3.1 Frequency scan technique	4
1.3.2 Eigenvalue analysis	5
1.3.3 Electromagnetic Transients Program (EMTP)	5
Chapter-2 Working Principle, Characteristics and modeling of TCSC	6
2.1 Introduction	6
2.2 Operation of TCSC	6
2.3 Different operating modes of a TCSC	7
2.3.1 Bypassed -Thyristor Mode	7
2.3.2 Blocked -Thyristor Mode	8
2.3.3 Partially Conducting Thyristor	8
2.3.4 Partially Conducting Thyristor	9
2.4 Impedance Vs Delay Angle characteristics of TCSC	10
2.5 Modeling of TCSC	11
2.6 Voltage and current waveforms of TCSC	14

Chapter-3	Modeling of TCSC compensated power system	16
	3.1 Test system	16
	3.2 Modeling for Electrical system	16
	3.3 Modeling for Mechanical system	19
	3.4 Controller Model	22
	3.4.1 Modeling of delay filter	23
	3.4.2 Modeling of PI controller	23
	3.4.3 Modeling of whole controller	24
	3.5 Modeling of the TCSC compensated network	25
	3.6 Combined model of electrical and mechanical system	26
	3.7 Complete System Modeling	27
Chapter-4	Results	30
	4.1 Introduction	30
	4.2 Eigen value analysis for SSR	30
	4.2.1 with capacitor as series compensator	30
	4.2.2 with TCSC as series compensator	31
	4.2. EMTDC/PSCAD Simulations	33
	4.2.1 with capacitor as series compensator	33
	4.2.2 with TCSC as series compensator	38
Chapter-5	Conclusion	43
	APPENDIX-A TEST SYSTEM PARAMETERS	44
	APPENDIX-B CALCULATION OF INITIAL CONDITIONS	46
	APPENDIX-C AC SYSTEM MODEL TRANSFORMATION FROM abc TO DQ0 CORDINATE	53
	APPENDIX-D SUB SYSTEMS MATRICES	55
	REFERENCES	62

## LIST OF FIGURES

---

		Page
Fig. 2.1	Block diagram of TCSC	6
Fig. 2.2	Variable inductor connected in shunt with fixed capacitor	
Fig. 2.3.1	Bypassed Thyristor Mode	7
Fig. 2.3.2	Blocked Thyristor Mode	8
Fig. 2.3.3	Partially Conducting Thyristor	8
Fig. 2.3.4	Partially Conducting Thyristor	9
Fig. 2.4	Impedance Vs Delay Angle characteristics of TCSC	10
Fig. 2.5	Modeling of TCSC	11
Fig. 2.6	A 3-ph source connected to 3-ph load through a TCSC	14
Fig. 2.7	Voltage and Current waveforms of TCSC in capacitive mode	15
Fig. 3.1	Test system	16
Fig. 3.3	Torsional system with six masses	19
Fig. 3.4	Controller model	22
Fig. 3.5	A TCSC compensated network	25
Fig. 4.3.1.1	HP to IP torque	33
Fig. 4.3.1.2	IP to LPA torque	33
Fig. 4.3.1.3	LPA to LPB Torque	34
Fig. 4.3.1.4	LPB to Generator torque	34

Fig. 4.3.1.5	Genarator to Excitor torque	35
Fig. 4.3.1.6	Smooth Electric torque	35
Fig. 4.3.1.7	Smooth Electric and frictional torque	36
Fig. 4.3.1.8	Electric torque negative	36
Fig. 4.3.1.9	Real power output	37
Fig. 4.3.1.10	Voltage across capacitor in ph-A	37



### 1.1 Introduction

In recent years, a greater demand has been placed on the transmission network, and these demands will increase because of the increase in the number of non-utility generators and the heightened competitions between the utilities themselves. Added to this is the problem that it is very difficult to acquire new rights of ways. Increased demands on transmission, absence of long term planning, and the need to provide open access to generating companies and customers, all together have created tendencies towards less security and reduced qualities of supplies. The FACTS technology is essential to alleviate some but not all these difficulties by enabling utilities to get their most services from their transmission facilities and provide grid reliability.

The operation of transmission parameters including series impedance, shunt impedance, current, voltage, damping of oscillations, phase angle, etc. at various frequencies below the rated frequency. By providing added flexibility, FACTS controller can enable a line carry power more closely to its thermal rating.

Some of the FACTS devices are SVC, TCSC, STATCOM, SSSC, UPFC etc.

SVC (Static var compensator) is a shunt-connected static var generator or absorber whose output is adjusted to exchange capacitive or inductive current so as to maintain or control specific parameters of the electrical power system (typically bus voltage).

TCSC (Thyristor controlled series capacitor) is a capacitive reactance compensator which consists of a series capacitor bank shunted by a thyristor controlled reactor in order to provide a smoothly variable series capacitive reactance.

STATCOM (Static synchronous compensator) is a static synchronous generator operated as a shunt-connected static var compensator whose capacitive or inductive output current can be controlled independent of the ac system voltage.

SSSC(Static synchronous series compensator) is a static synchronous generator operated without an external electric energy source as a series compensator whose

output voltage is in quadrature with ,and controllable independently of ,the line current for the purpose of increasing or decreasing the overall reactive voltage drop across the line and thereby controlling the transmitted electric power.

UPFC (Unified power-flow controller) is a combination of a STATCOM and a SSSC which are coupled via a common dc link, to allow bidirectional flow of real power between series output terminals of the SSSC and the shunt output terminals of the STATCOM, and are controlled to provide concurrent real and reactive series line compensation without an external electric energy source.

Series capacitor compensation in A.C. transmission systems can yield several benefits; such as increased power transfer capability and enhancement transient stability. However in long transmission line it can lead to Subsynchronous resonance (SSR), which is a serious threat to our power system. In this dissertation we solely study the SSR analysis of TCSC (thyristor controlled series capacitor) compensated power system.

## 1.2 Subsynchronous resonance (SSR)

Subsynchronous resonance is an electric power system condition where the electric network exchanges energy with a turbine generator at one or more of the natural frequencies of the combined system below the synchronous frequency of the system. Such SSR and associated turbine-generator torsional interactions are an instability in which the large subsynchronous torques. There are many ways in which the system and the generator may interact with subsynchronous effects. But three are of particular interest as Induction Generator Effect, Torsional Interaction Effect and Transient Torque Effect.

### 1.2.1 Induction Generator Effect

Induction generator effect is caused by self-excitation of the electrical system. The resistance of the rotor to subsynchronous current, viewed from the armature terminals, is a negative resistance. The network also presents a resistance to these same currents

that is positive. However, if the negative resistance of the generator is greater in magnitude than the positive resistance of the network at the system natural frequencies, there will be sustained subsynchronous currents. This is the condition known as the "induction generator effect."

### 1.2.2 Torsional Interaction Effect

Torsional interaction occurs when the induced subsynchronous torque in the generator is close to one of the torsional natural modes of the turbine-generator shaft. When this happens, generator rotor oscillations will build up and this motion will induce armature voltage components at both subsynchronous and super synchronous frequencies. Moreover, the induced subsynchronous frequency voltage is phased to sustain the subsynchronous torque. If this torque equals or exceeds the inherent mechanical damping of the rotating system, the system will become self-excited. This phenomenon is called "torsional interaction."

### 1.2.3 Transient Torque Effect

Transient torques are those that result from system disturbances. System disturbances cause sudden changes in the network, resulting in sudden changes in currents that will tend to oscillate at the natural frequencies of the network. In a transmission system without series capacitors, these transients are always dc transients, which decay to zero with a time constant that depends on the ratio of inductance to resistance. For networks that contain series capacitors will contain one or more oscillatory frequencies that depend on the network capacitance as well as the inductance and resistance. In a simple radial R-L-C system, there will be only one such natural frequency, but in a network with many series capacitors there will be many such subsynchronous frequencies. If any of these subsynchronous network frequencies coincide with one of the natural modes of a turbine-generator shaft, there can be peak torques that are quite large since these torques are directly proportional to the magnitude of the oscillating current. Currents due to short circuits, therefore, can

produce very large shaft torques both when the fault is applied and also when it is cleared. In a real power system there may be many different subsynchronous frequencies involved and the analysis is quite complex. From the viewpoint of system analysis, it is important to note that the induction generator and torsional interaction effects may be analyzed using linear models, suggesting that eigenvalue analysis is appropriate for the study of these problems. There are several analytical tools that have evolved for the study of SSR. The most common of these tools will be described briefly.

### 1.3.1 Frequency scan technique

The frequency scan technique computes the equivalent resistance and inductance, seen looking into the network from a point behind the stator winding of a particular generator, as a function of frequency. Should there be a frequency at which the inductance is zero and the resistance negative, self sustaining oscillations at that frequency would be expected due to induction generator effect.

It also provides information regarding possible problems with torsional interaction and transient torques which might be expected to occur if there is a network series resonance or a reactance minimum that is very close to one of the shaft torsional frequencies.

Since the frequency scan results change with different system conditions and with the number of generators on line, many conditions need to be tested. Frequency scanning is limited to the impedances seen at a particular point in the network, usually behind the stator windings of a generator. The process must be repeated for different system (switching) conditions at the terminals of each generator of interest.

### 1.3.2 Eigenvalue analysis

Eigenvalue analysis provides additional information regarding the system performance. This type of analysis is performed with the network and the generators modeled in one linear system of differential equations. The results give both the frequencies of oscillation as well as the damping of each frequency.

### 1.3.3 Electromagnetic Transients Program (EMTP)

The Electromagnetic Transients Program (EMTP) is a program for numerical integration of the system differential equations. Unlike a transient stability program, which usually models only positive sequence quantities representing a perfectly balanced system, EMTP is a full three-phase model of the system with much more detailed models of transmission lines, cables, machines, and special devices such as series capacitors with complex bypass switching arrangements. Moreover, the EMTP permits nonlinear modeling of complex system components. It is, therefore, well suited for analyzing the transient torque SSR problems. EMTP adds important data on the magnitude of the oscillations as well as their damping.

Flexible A.C. transmission system such as thyristor controlled series capacitor (TCSC), offer the possibility of power flow control and suppression of SSR instabilities through controlled series compensation. This report examines the SSR behavior of the thyristor compensated power system using eigenvalue method and compares the SSR performance with a fixed capacitor compensated system. The IEEE first benchmark model for SSR is used as the test system for eigenvalue analysis.

The report is organized as follows: Chapter 2 describes the details about TCSC, its characteristics. Chapter 3 contains the models of electromechanical system and network equations, then these individual subsystems are combined to get overall model of the TCSC compensated power system, and the computation of the eigenvalues. Chapter 4 contains the results of our eigenvalue analysis and results of PSCAD/EMTDC simulations. Finally Chapter 5 is about conclusion.

### 2.1 Introduction

A Thyristor controlled series capacitor (TCSC) is a capacitive reactance compensator which consists of a series capacitor bank shunted by a thyristor controlled reactor (TCR : A shunt connected, thyristor-controlled inductor whose effective reactance is varied in a continuous manner by partial-conduction control of the thyristor) in order to provide a smoothly variable series capacitive reactance. TCSCs are expected to provide many benefits for an electric power system including the increase of power transfer capability and transient stability as well as the mitigation of sub synchronous resonance (SSR).

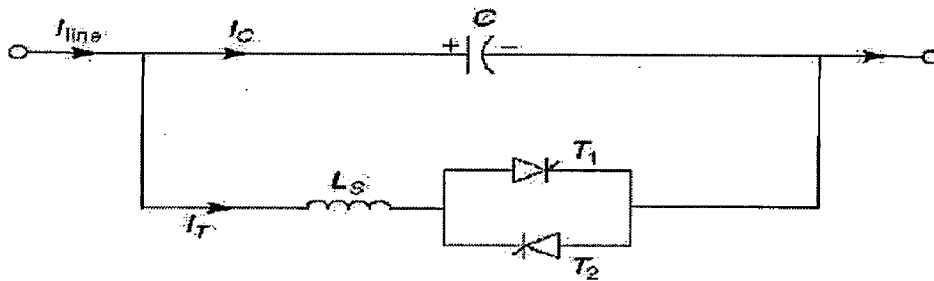


Fig 2.1 Block diagram of TCSC

In the figure 2.1,  $I_{line}$ ,  $I_C$ ,  $I_T$ ,  $L_s$ ,  $C$ ,  $T_1$  and  $T_2$  are the line current, current flowing through the capacitor, inductor and the capacitor, the thyristors used in bidirectional way.

### 2.2 Operation of TCSC

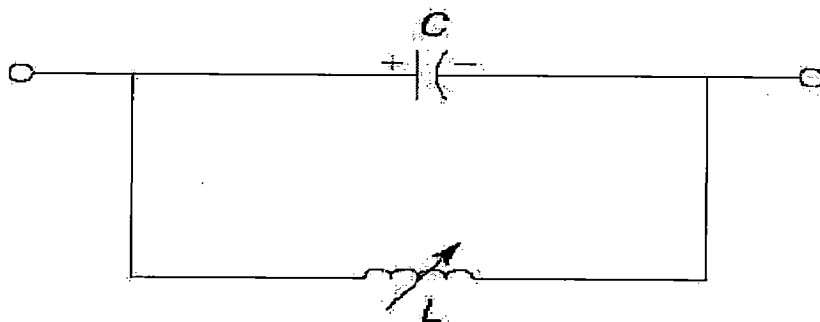


Fig.2.2 (A variable inductor connected in shunt with fixed capacitor)

From the system point of view TCSC (Fig. 2.2) which provides variable-series compensation is simply to increase the fundamental-frequency voltage across a fixed capacitor in a series compensated line through appropriate variation of firing angle  $\alpha$ . This enhanced voltage changes the effective value of the series-capacitive reactance. The equivalent impedance is

$$Z_{eq} = \left(-j\frac{1}{\omega C}\right) \parallel (j\omega L) = -j\frac{1}{\omega C - \frac{1}{\omega L}}$$

If  $\omega C - \frac{1}{\omega L} > 0$ , or  $\omega L > \frac{1}{\omega C}$ , the reactance of fixed capacitor is less than that of the parallel connected variable reactor and this combination provides a variable capacitive reactance. Moreover, this inductor increases the equivalent capacitive reactance of the LC combination above that of the fixed capacitor.

If  $\omega C - \frac{1}{\omega L} = 0$ , a resonance condition results which leads to infinite capacitive impedance. This is obviously unacceptable.

If  $\omega C - \frac{1}{\omega L} < 0$ , the LC combination provides a variable inductance above the value of fixed inductor. This situation corresponds to inductive Vernier mode of TCSC operation.

### 2.3 Different operating modes of a TCSC:

#### 2.3.1 Bypassed -Thyristor Mode :

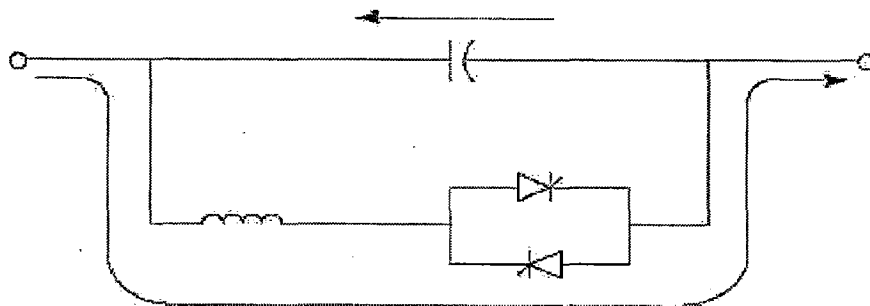


Fig 2.3.1 Bypassed -Thyristor Mode

Thyristor are made fully conductive by a conduction angle of 180 as in Fig. 2.3.1.

As soon as the voltage across thyristor becomes zero and advances towards positive gate pulses are applied and this results a sinusoidal flow of current through the thyristor. That implies the net impedance is reactive. Thus the thyristor behaves as if a parallel combination of inductor and capacitor.

2.3.2 Blocked -Thyristor Mode:

In this blocking command is given to thyristor & as soon as the current through the thyristor reaches to 0, these turn off. This implies TCSC reduces to a capacitor. This is shown in Figure 2.3.2

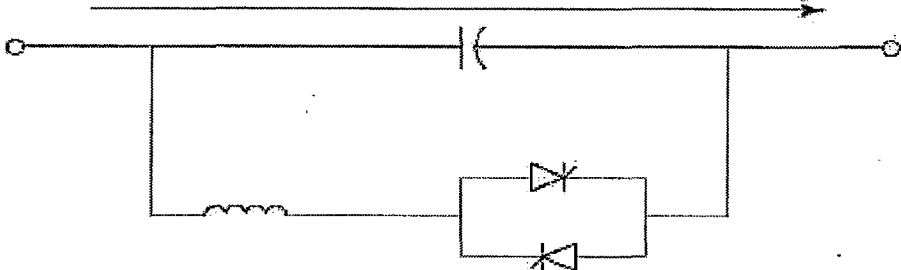


Fig 2.3.2 Blocked -Thyristor Mode

2.3.3 Partially Conducting Thyristor (Capacitive Vernier Mode):

In this we are trying the TCSC to behave as continuous reactor or inductor. This is achieved by varying the thyristor pair firing angle in a particular range. But a smooth transition from inductive to capacitive is not possible because of the resonant region between the two.

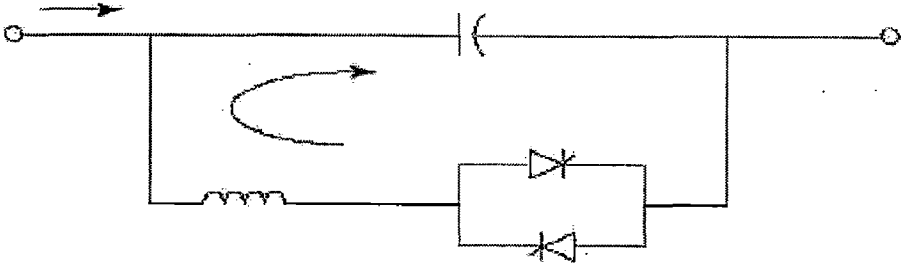


Fig. 2.3.3 Partially Conducting Thyristor (Capacitive Vernier Mode)



When the voltage & current across the capacitance are in opposite direction thyristor are fired, this causes a loop current flow which adds up with the line current through the capacitance causing a net capacitance voltage drop which is more than its normal value, and this implies that we have made our TCSC to operate in a capacitive mode.  $\alpha$  is a delay angle measured from the crest of the capacitor voltage or from the zero crossing of the line current.

2.3.4 Partially Conducting Thyristor (Inductive Vernier Mode):

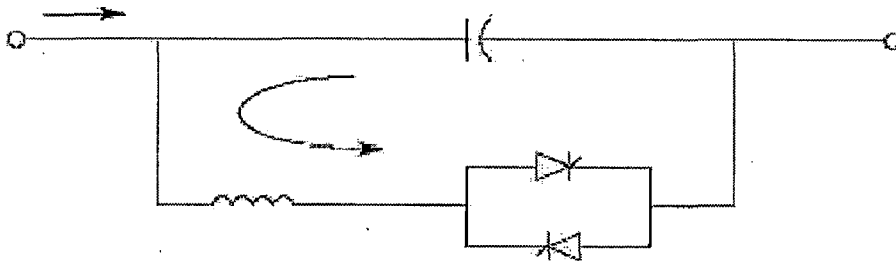


Fig 2.3.4 Partially Conducting Thyristor (Inductive Vernier Mode)

We can explain this mode just as opposite to previous mode. In this the loop current flows in opposite direction. When the voltage & current across the capacitance are in same direction thyristors are fired, this causes a loop current flow which acts in opposite direction to the line current through the capacitance causing a net capacitance voltage drop which is less than its normal value, this implies that we have made our TCSC to operate in an inductive mode.

## 2.4 Impedance Vs Delay Angle characteristics of TCSC:

The internal operation of TCSC can be understood by the following Impedance Vs delay angle characteristics.

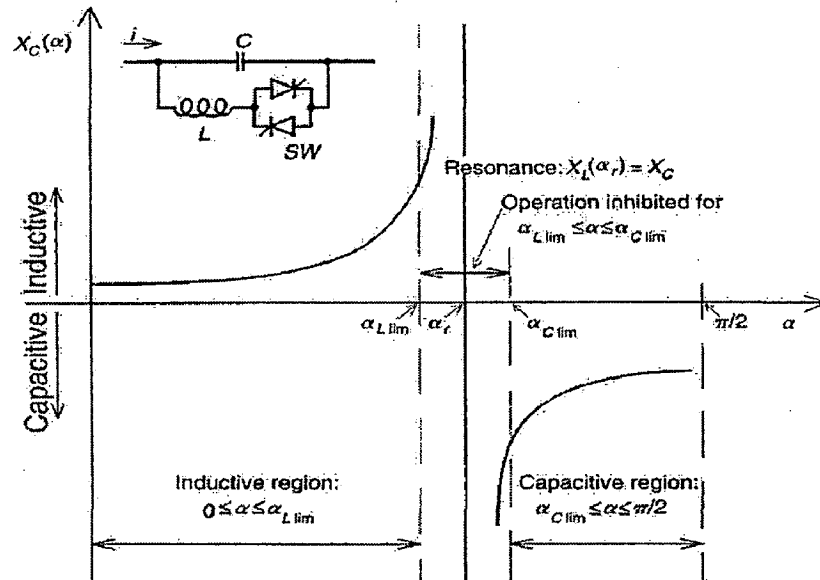


Fig. 2.4 Impedance Vs Delay Angle characteristics of TCSC

At the resonant point, the TCSC exhibits very large impedance and results in a significant voltage drop. This region is avoided by installing limits on the firing angle. TCSC presents a constant alternating current source. As the impedance of the reactor is  $X_L(\alpha)$ , is varied from its maximum (infinity) towards its minimum ( $\omega L$ ), the TCSC increases its minimum capacitive impedance,  $X_{TCSC, \min} = X_C = \frac{1}{\omega C}$ , until parallel resonance occurs at  $X_C = X_L(\alpha)$  is established and  $X_{TCSC, \max}$  theoretically becomes infinity. Decreasing  $X_L(\alpha)$  further, the impedance of the TCSC,  $X_{TCSC}(\alpha)$  becomes inductive, reaching its minimum value of  $X_L X_C / (X_L - X_C)$  at  $\alpha = 0$ , where the capacitor is in effect bypassed by the TCR. So with the usual TCSC arrangement in which the impedance of the TCR reactor,  $X_L$ , is smaller than of the capacitor,  $X_C$ , the TCSC has 2 operating ranges around its internal circuit resonance: one is the  $\alpha_C \lim \leq \alpha \leq \pi/2$ , where  $X_{TCSC}(\alpha)$  is inductive. The dynamic interaction between

capacitor and reactor changes the operating voltage from that of the basic sine wave established by the constant line current.

### 2.5 Modeling of TCSC

The fundamental frequency model of a TCSC is derived first to enable initialization of the steady-state parameters. The voltage across the TCSC capacitor  $v_c$  comprises an uncontrolled and a controlled component and it is presumed that the line current is constant over one fundamental cycle in accordance with [2], [3], [8]. The uncontrolled component  $v_1$  is a *sine* wave (unaffected by thyristor switching) and it is also constant over a fundamental cycle since it is directly related to the amplitude of the prevailing line current. The controlled component  $v_2$  is a nonlinear variable that depends on circuit variables and on the TCR firing angle. In this study, the controlled component is represented as a nonlinear function of the uncontrolled component and firing angle,  $v_2 = N_1(v_1, \alpha, s)$ , as shown in Fig. below. With this approach,  $N_1(v_1, \alpha, s)$  captures the nonlinear phenomena caused by thyristor switching influence and all internal interactions with capacitor voltage assuming only that the line current and  $v_1$  are linear. We seek in our work to study dynamics of  $N_1(v_1, \alpha, s)$  in a wider frequency range and also to offer a simplified representation for fundamental frequency studies.

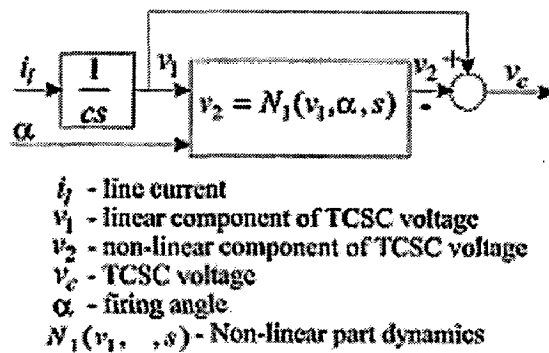


Fig. 2. 5. TCSC model

The following transfer function is proposed

$$\frac{v_2(s)}{v_1(s)} = \frac{\frac{s^2}{\omega_n^2} + \frac{2\zeta_n s}{\omega_n} + 1}{\frac{s^2}{\omega_d^2} + \frac{2\zeta_d s}{\omega_d} + 1} \quad (2.1)$$

Where the unknown constants are

$$\omega_d = \frac{\pi - 2\alpha}{\pi \sqrt{I_{cr} c}}$$

$$\zeta_d = 0.38 \cos(\alpha)$$

$$\omega_n = \frac{\pi f_0 10^{-3}}{\sqrt{I_{cr} c}} \left( 1.7 + \sqrt{10} \frac{\alpha}{\tan 4(\alpha)} \right)$$

$$\zeta_n = 0.2 \cos(\alpha)$$

The model 2.5 is next transferred into state-space domain

$$\dot{x}_1 = \frac{i_l}{C}$$

$$\dot{x}_2 = x_3$$

$$\dot{x}_3 = \omega_d^2 x_1 - \omega_d^2 x_2 - \omega_d \zeta_d x_3$$

$$\dot{x}_4 = \frac{1}{T_f} \left( 1 - \frac{\omega_d^2}{\omega_n^2} \right) x_1 + \frac{1}{T_f} \left( \frac{\omega_d}{\omega_n^2} - 1 \right) x_2 + \frac{1}{T_f} \left( \frac{\omega_d \zeta_d}{\omega_n^2} - \frac{\zeta_n}{\omega_n} \right) x_3 + \frac{1}{T_f} x_4$$

Applying D-Q transformations to the above equations we got

$$\dot{x}_{1D} + \omega_0 x_{1Q} = \frac{i_D}{C}$$

$$\dot{x}_{2D} + \omega_0 x_{2Q} = x_{3D}$$

$$\dot{x}_{3D} + \omega_0 x_{3Q} = \omega_d^2 x_{1D} - \omega_d^2 x_{2D} - \omega_d \zeta_d x_{3D}$$

$$\dot{x}_{4D} + \omega_0 x_{4Q} = \frac{1}{T_f} \left( 1 - \frac{\omega_d^2}{\omega_n^2} \right) x_{1D} + \frac{1}{T_f} \left( \frac{\omega_d}{\omega_n^2} - 1 \right) x_{2D} + \frac{1}{T_f} \left( \frac{\omega_d \zeta_d}{\omega_n^2} - \frac{\zeta_n}{\omega_n} \right) x_{3D} + \frac{1}{T_f} x_{4D}$$

$$\dot{x}_{1Q} - \omega_0 x_{1D} = \frac{i_Q}{C}$$

$$\dot{x}_{2Q} - \omega_0 x_{2D} = x_{3Q}$$

$$\dot{x}_{3Q} - \omega_0 x_{3D} = \omega_d^2 x_{1Q} - \omega_d^2 x_{2Q} - \omega_d \zeta_d x_{3Q}$$

$$\dot{x}_{4Q} - \omega_0 x_{4D} = \frac{1}{T_f} \left( 1 - \frac{\omega_d^2}{\omega_n^2} \right) x_{1Q} + \frac{1}{T_f} \left( \frac{\omega_d}{\omega_n^2} - 1 \right) x_{2Q} + \frac{1}{T_f} \left( \frac{\omega_d \zeta_d}{\omega_n^2} - \frac{\zeta_n}{\omega_n} \right) x_{3Q} + \frac{1}{T_f} x_{4Q}$$

$$\dot{x}_{1D} = -\omega_0 x_{1Q} + \frac{i_D}{C} \quad (2.2)$$

$$\dot{x}_{2D} = -\omega_0 x_{2Q} + x_{3D} \quad (2.3)$$

$$\dot{x}_{3D} = -\omega_0 x_{3Q} + \omega_d^2 x_{1D} - \omega_d^2 x_{2D} - \omega_d \zeta_d x_{3D} \quad (2.4)$$

$$\dot{x}_{4D} = -\omega_0 x_{4Q} + \frac{1}{T_f} \left( 1 - \frac{\omega_d^2}{\omega_n^2} \right) x_{1D} + \frac{1}{T_f} \left( \frac{\omega_d}{\omega_n^2} - 1 \right) x_{2D} + \frac{1}{T_f} \left( \frac{\omega_d \zeta_d}{\omega_n^2} - \frac{\zeta_n}{\omega_n} \right) x_{3D} + \frac{1}{T_f} x_{4D} \quad (2.5)$$

$$\dot{x}_{1Q} = \omega_0 x_{1D} + \frac{i_Q}{C} \quad (2.6)$$

$$\dot{x}_{2Q} = \omega_0 x_{2D} + x_{3Q} \quad (2.7)$$

$$\dot{x}_{3Q} = \omega_0 x_{3D} + \omega_d^2 x_{1Q} - \omega_d^2 x_{2Q} - \omega_d \zeta_d x_{3Q} \quad (2.8)$$

$$\dot{x}_{4Q} = \omega_0 x_{4D} + \frac{1}{T_f} \left( 1 - \frac{\omega_d^2}{\omega_n^2} \right) x_{1Q} + \frac{1}{T_f} \left( \frac{\omega_d}{\omega_n^2} - 1 \right) x_{2Q} + \frac{1}{T_f} \left( \frac{\omega_d \zeta_d}{\omega_n^2} - \frac{\zeta_n}{\omega_n} \right) x_{3Q} + \frac{1}{T_f} x_{4Q} \quad (2.9)$$

## 2.6 Voltage and current waveforms of TCSC

The figure shown below is a TCSC connected between a 3-ph source and a 3-ph load.

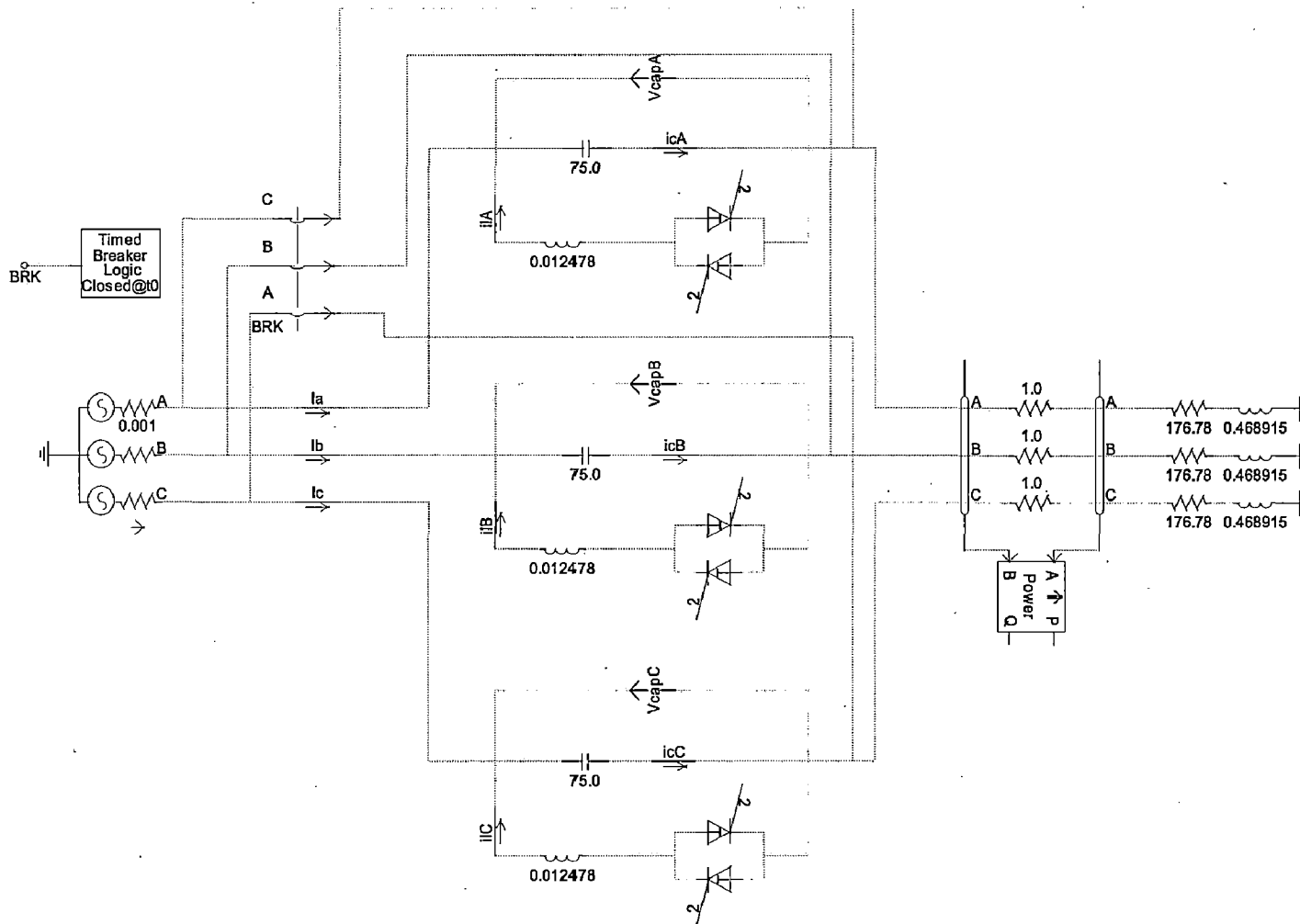


Fig. 2.6 A 3-ph source connected to 3-ph load through a TCSC

The line current, current through capacitor and inductor in the capacitor mode is given below:

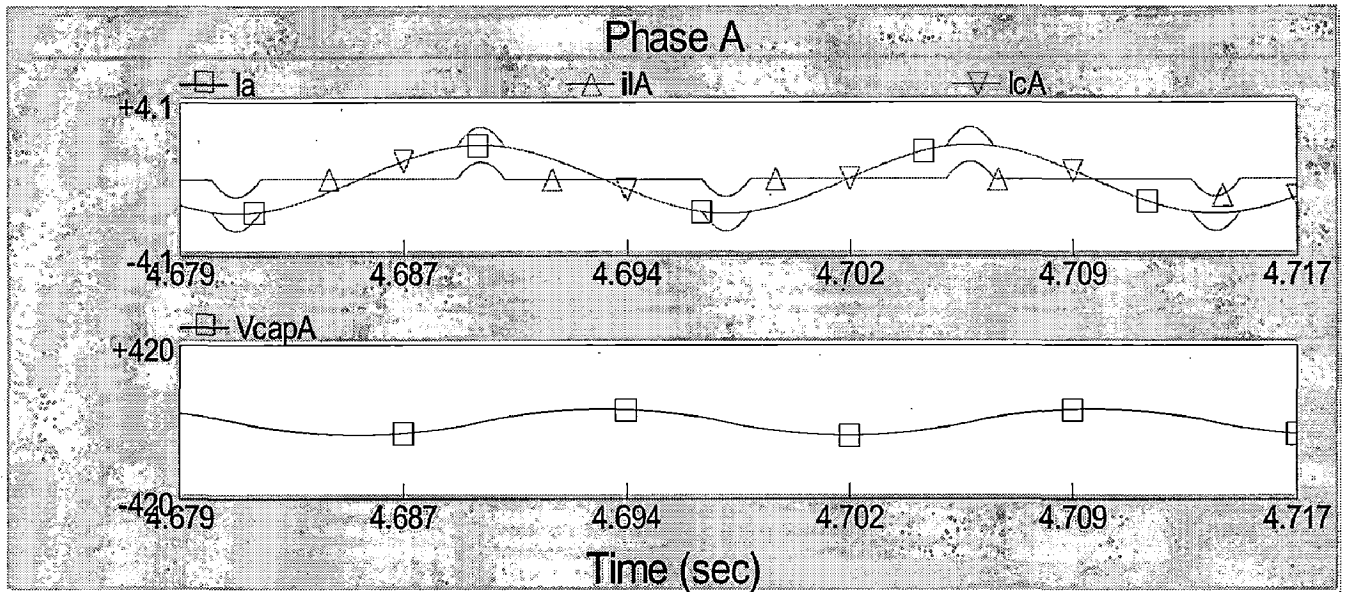


Fig. 2.7 Voltage and Current waveforms of TCSC in capacitive mode

In the capacitive mode, when thyristor is turned on the current through the inductor added up with the original current flowing through the capacitor resulting a higher voltage across the capacitor

### 3.1 Test system

The system for the SSR study should be modeled more in detail than that of the low frequency oscillation study. So the complete SSR simulation system based on the IEEE first benchmark is employed for this study. As shown in Fig. 3.1, this system consists of one synchronous generator which is connected to the infinite bus through a series compensated transmission line and a governor-turbine system which is expressed as a spring-mass system.

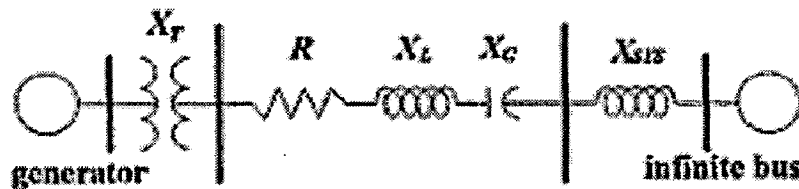


Fig. 3.1 Test system

### 3.2 Modeling of Electrical system

The voltage equations of the stator and rotor coils are given below.

$$-\frac{d\phi_s}{dt} - [R_s]i_s = v_s \quad (3.1)$$

$$-\frac{d\phi_r}{dt} - [R_r]i_r = v_r \quad (3.2)$$



where

$$V_s^t = [V_a \quad V_b \quad V_c]$$

$$V_r^t = [-V_f \quad 0 \quad 0 \quad 0]$$

$$[R_s] = \begin{bmatrix} R_a & 0 & 0 \\ 0 & R_a & 0 \\ 0 & 0 & R_a \end{bmatrix}$$

$$[R_r] = \begin{bmatrix} R_f & 0 & 0 & 0 \\ 0 & R_f & 0 & 0 \\ 0 & 0 & R_f & 0 \\ 0 & 0 & 0 & R_f \end{bmatrix}$$

The combined voltage equations (for stator and rotor) can be expressed as

$$\frac{d\phi}{dt} = -[R][L]^{-1}\phi - v$$

$$i = [L]^{-1}\phi$$

Where

$$[L] = \begin{bmatrix} L_{ss} & L_{sr} \\ L_{rs} & L_{rr} \end{bmatrix}$$

$$[R] = \begin{bmatrix} R_s & 0 \\ 0 & R_r \end{bmatrix}$$

$$\phi^t = [\phi_s^t \quad \phi_r^t]$$

$$i^t = [i_s^t \quad i_r^t]$$

$$v^t = [v_s^t \quad v_r^t]$$

Applying the Park's transformation as

$$[f_a \quad f_b \quad f_c]^t = [C_p][f_d \quad f_q \quad f_0]^t$$

Where  $f_\alpha$  can be either stator voltage, current or flux linkage of the stator winding and

$\alpha$  can be a, b, c.  $[C_p]$  is defined by

$$[C_p] = \begin{bmatrix} k_d * \cos \theta & k_q * \sin \theta & k_0 \\ k_d * \cos(\theta - \frac{2\pi}{3}) & k_d * \sin(\theta - \frac{2\pi}{3}) & k_0 \\ k_d * \cos(\theta - \frac{4\pi}{3}) & k_d * \sin(\theta - \frac{4\pi}{3}) & k_0 \end{bmatrix}$$

Where  $k_d, k_q, k_0$  are constants as 1, -1, 1.

The inverse transformation is given by

$$[f_d \ f_q \ f_0]^t = [C_p]^{-1} * [f_a \ f_b \ f_c]$$

Applying Park's transformation 3.1 can be rewritten as

$$-\frac{d}{dt}[C_p \varphi_{dq0}] - [R_s][C_p]i_{dq0} = [C_p]v_{dq0}$$

This can be written as

$$-\frac{d\phi_d}{dt} - \dot{\theta} \frac{k_q}{k_d} \varphi_q - Ri_d = v_d \quad (3.3)$$

$$-\frac{d\phi_q}{dt} - \dot{\theta} \frac{k_d}{k_q} \varphi_d - Ri_q = v_q \quad (3.4)$$

Where  $\omega = \dot{\theta} = \omega_0$  in steady state .Subscript 0 indicates the value at the operating point.

Now the stator equations can be written as

$$-\frac{1}{\omega_B} \rho \phi_d - (1 + S_m) \phi_d - Ri_d = v_d \quad (3.5)$$

$$-\frac{1}{\omega_B} \rho \phi_q - (1 + S_m) \phi_q - Ri_q = v_q \quad (3.6)$$

The rotor electrical equations are written as (assuming machine model 1.1, [1])

$$\rho E_d' = \frac{1}{T_{q0}} [-E_d' - (x_q - x_q') i_q] \quad (3.7)$$

$$\rho E_q' = \frac{1}{T_{d0}} [-E_q' - (x_d - x_d') i_d + E_{fd}] \quad (3.8)$$

So finally the electrical system state equations can be written as

$$\dot{x}_e = [A_e]x_e + [B_{e1}]u_e + [B_{e2}]E_{fd}$$

$$y_e = [C_e]x_e$$

$$\text{where } x_e^t = [\varphi_d \ \varphi_q \ E_d' \ E_q']$$

$$u_e^t = [V_D \ V_Q]$$

$$y_e^t = [i_D \ i_Q]$$

Where all the unknown matrices are given in the appendix D

### 3.3 Modeling of Mechanical system

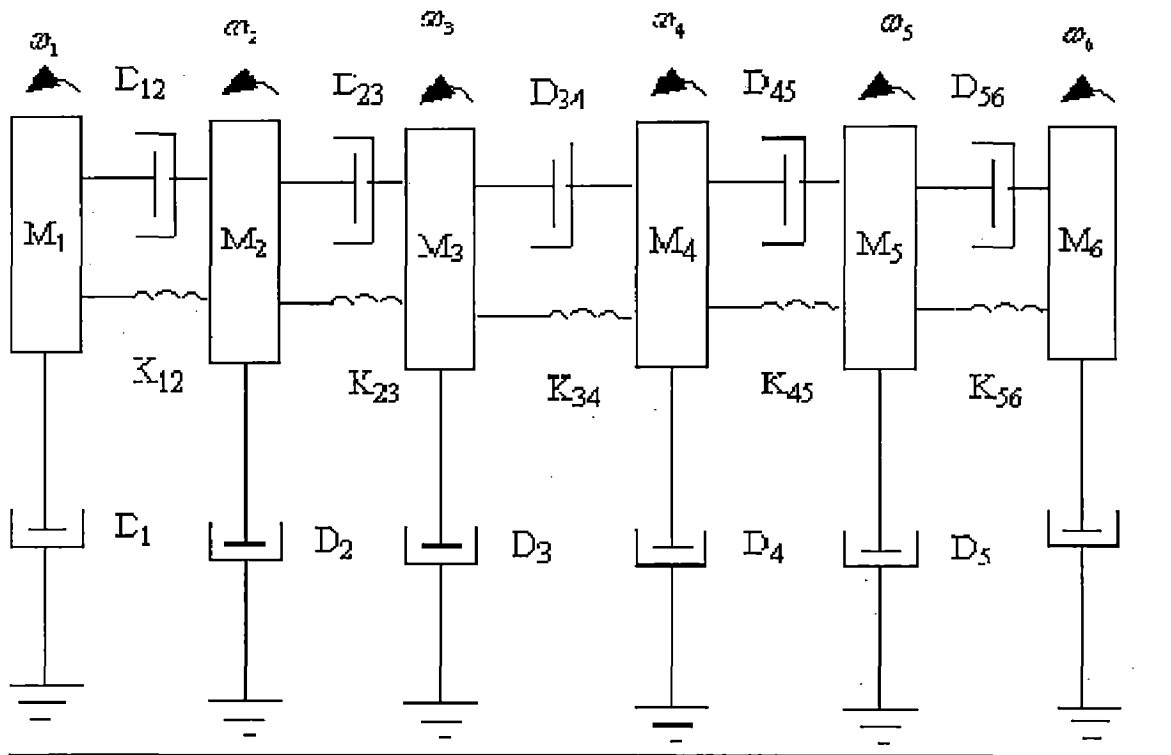


Fig.3.3 Torsional system with six masses

The mechanical system consists of rotors of generator, exciter and turbines, shafts can be viewed as mass-spring-damper system. The mechanical system equations can be written as an analogy to an electrical network (RLC) network.

Defining per unit slip of a mass ( $M_i$ ) as

$$S_i = \frac{\omega_i - \omega_B}{\omega_B}$$

We can express

$$\frac{d\delta_i}{dt} = \omega_B (S_i - S_{i_0})$$

$$2H_i \frac{dS_i}{dt} + D_i (S_i - S_{i_0}) + D_{i,i-1} (S_i - S_{i-1}) + D_{i,i+1} (S_i - S_{i+1}) + T_{i,i-1} + T_{i,i+1} = T_{mi} - T_{ei}$$

$$\frac{dT_{i,i-1}}{dt} = K_{i,i-1} (S_i - S_{i-1}) \omega_B$$

$$\frac{dT_{i,i+1}}{dt} = K_{i,i+1} (S_i - S_{i+1}) \omega_B$$

Where  $T_{i,i-1}$  is the torque in the shaft section connecting mass  $i$  and  $i-1$  and  $2H$  is analogous to a capacitance, slip analogous to voltage and torque as current. The p.u. damping co-efficient as conductances.

The state variables for this system are given by

$$X_m^t = [S_1 \ S_2 \ S_3 \ S_4 \ S_5 \ S_6 \ T_{12} \ T_{23} \ T_{34} \ T_{45} \ T_{56}]$$

The additional state variable required for writing equations for the electrical system is  $\delta_m$  i.e., rotor angle corresponding to the generator rotor. The equation for it is given by

$$\frac{d\delta_m}{dt} = \omega_B (S_m - S_{m_0})$$

Where  $S_m$  is the generator rotor slip.

The mechanical system state equation can be written as

$$\begin{aligned}\dot{x}_m &= [A_m]x_m + [B_{m1}]T_e + [B_{m2}]u_m \\ y_m &= [C_m]x_m\end{aligned}$$

Where  $u_m$  is equal to the vector of mechanical torques applied at different turbine rotors, if prime movers dynamics are not included in the equations. If turbine-generator dynamics are to be included,  $u_m$  is the input variable corresponding to the speed reference.  $T_e$  is the electromagnetic torque of the generator applied at the generator rotor mass.

For the 6-mass system the state vector given by

$$X_m' = [ \delta \quad S_{exc} \quad T_{LGE} \quad S_m \quad T_{LBG} \quad S_{LPB} \quad T_{ILPAB} \quad S_{LPA} \quad T_{ILPA} \quad S_{IP} \quad T_{HI} \quad S_{HP} ]$$

Where  $T_{LGE}, T_{LBG}, T_{ILPAB}, T_{ILPA}, T_{HI}, S_m, S_{LPB}, S_{LPA}, S_{IP}$  are the shaft torques and the rotor slips of different rotors and  $\delta$  is the generator rotor angle.

Although the mechanical system equations are linear, the coupling between the mechanical and electrical equations are non-linear. Hence it is required to linearize the equations for small signal stability analysis.

### 3.4 Controller Model

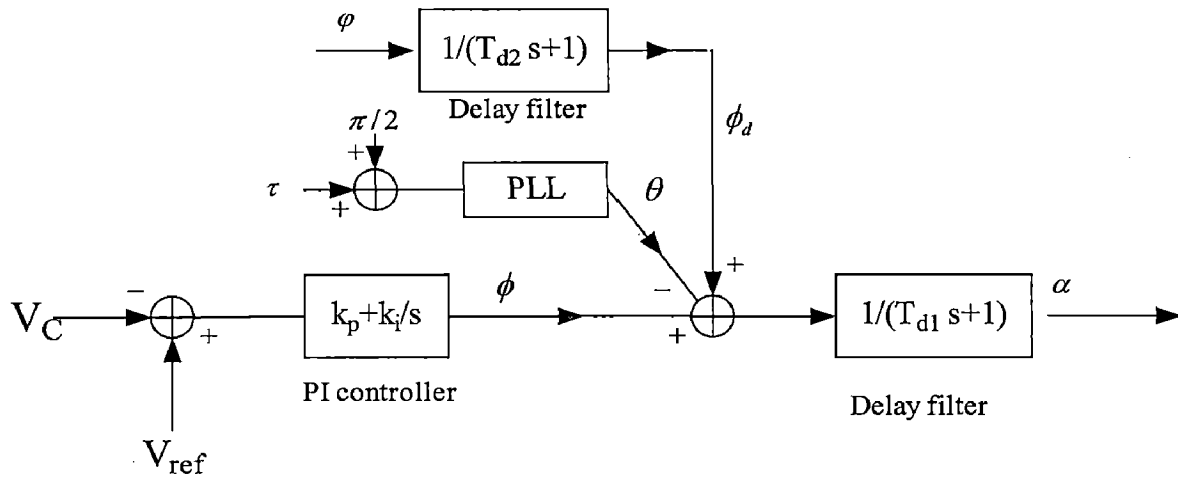


Fig.3.4 Controller model

- $V_C$  -- Voltage across capacitor     $\tau$  --line current angle  
 $V_{ref}$ --reference voltage         $\phi$  --voltage angle  
 $\alpha$  --actual firing angle

The controller model consists of a PI controller, PLL, series compensator and 2 transport delay model, as shown in Fig. 3.4. The PLL system is of the d-q -z type. The state-space linearized second-order PLL model is developed in [11]. The PLL synchronizes thyristor firings with the line current phase angle. For simplicity reasons, the TCSC voltage feedback control is used where  $V_{ref}$  can be a function of other parameters at higher control levels. Because of the thyristor firings at discrete time instants the system is actually a sampled data system with the sampling frequency  $f_s=360\text{Hz}$ . The continuous model, therefore, includes a first-order delay, given by time constant  $T_{d1}$  to accommodate the phase lag introduced by sampling the firing angle signal. The filter time constant is of the order of 2 ms, which is in line with other studies. It should be noted that the voltage phase angle also affects the

firing angle because the actual firing angle is measured with respect to the voltage curve. Here, we have direct correlation across each phase, and the sampling frequency is 1/3 of  $f_s$  and, therefore, an additional lag is introduced represented by the delay filter with. Simulation results demonstrate improvement in the response with the introduction of this delay element.

### 3.4.1 Modeling of delay filter

$$\begin{aligned} \varphi \left( \frac{1}{T_{d2}s + 1} \right) &= x_7 \\ \varphi &= T_{d2}s * x_7 + x_7 \\ sx_7 &= \frac{\varphi}{T_{d2}} - \frac{x_7}{T_{d2}} \\ \dot{x}_7 &= -\frac{1}{T_{d2}}x_7 + \frac{\varphi}{T_{d2}} \end{aligned} \tag{3.9}$$

### 3.4.2 Modeling of PI controller

$$V_C^2 = V_{CD}^2 + V_{CQ}^2$$

Taking differential of both sides

$$2V_C \Delta V_C = 2V_{CD} \Delta V_{CD} + 2V_{CQ} \Delta V_{CQ}$$

$$\Delta V_C = \frac{V_{CD0}}{V_{C0}} \Delta V_{CD} + \frac{V_{CQ0}}{V_{C0}} \Delta V_{CQ}$$

$$\Delta x_4 = \frac{x_{4D0}}{x_{40}} \Delta x_{4D} + \frac{x_{4Q0}}{x_{40}} \Delta x_{4Q}$$

$$\Delta \dot{x}_4 = \frac{x_{4D0}}{x_{40}} \Delta \dot{x}_{4D} + \frac{x_{4Q0}}{x_{40}} \Delta \dot{x}_{4Q}$$

Putting (3.26) & (3.24) in (3.25) we got

$$\begin{aligned}\Delta u_G &= \Delta x_{N1} + [F][C_G]\Delta x_G + \frac{x_L}{w_b} [[C_G A_G]\Delta x_G + [C_G B_G]\Delta u_G] \\ \Delta u_G &= \Delta x_{N1} + [F][C_G]\Delta x_G + \frac{x_L}{w_b} [C_G A_G]\Delta x_G + \frac{x_L}{w_b} [C_G B_G]\Delta u_G \\ \Delta u_G \left[ 1 - \frac{x_L}{w_b} [C_G B_G] \right] &= \Delta x_{N1} + \left[ [F][C_G] + \frac{x_L}{w_b} [C_G A_G] \right] \Delta x_G \\ \Delta u_G &= \left[ 1 - \frac{x_L}{w_b} [C_G B_G] \right]^{-1} \left[ \Delta x_{N1} + \left[ [F][C_G] + \frac{x_L}{w_b} [C_G A_G] \right] \Delta x_G \right] \\ \Delta u_G &= \left[ 1 - \frac{x_L}{w_b} [C_G B_G] \right]^{-1} \Delta x_{N1} + \left[ 1 - \frac{x_L}{w_b} [C_G B_G] \right]^{-1} \left[ [F][C_G] + \frac{x_L}{w_b} [C_G A_G] \right] \Delta x_G\end{aligned}$$

$$\text{Let } H = \left[ 1 - \frac{x_L}{w_b} [C_G B_G] \right]^{-1}$$

Now

$$\Delta u_G = [H]\Delta x_{N1} + [H] \left[ [F][C_G] + \frac{x_L}{w_b} [C_G A_G] \right] \Delta x_G \quad (3.27)$$

Putting (3.27) in (3.23) we got

$$\begin{aligned}\Delta \dot{x}_G &= [A_G]\Delta x_G + [B_G]\Delta u_G \\ \Delta \dot{x}_G &= [A_G]\Delta x_G + [B_G][H]\Delta x_{N1} + [B_G][H] \left[ [F][C_G] + \frac{x_L}{w_b} [C_G A_G] \right] \Delta x_G \\ \Delta \dot{x}_G &= \left[ [A_G] + [B_G][H] \left[ [F][C_G] + \frac{x_L}{w_b} [C_G A_G] \right] \right] \Delta x_G + [B_G][H]\Delta x_{N1}\end{aligned}$$

Let

$$\begin{aligned}L &= \left[ [A_G] + [B_G][H] \left[ [F][C_G] + \frac{x_L}{w_b} [C_G A_G] \right] \right] \\ \Delta \dot{x}_G &= L\Delta x_G + [B_G][H]\Delta x_{N1}\end{aligned}$$

From (3.15) & (3.16) the linearized network equations are

$$\begin{aligned}\Delta \dot{x}_{N1} &= [A_{N1}]\Delta x_{N1} + [D_{N1}]\Delta x_{N2} + [B_{N1}]\Delta u_{N1} + [B_{N2}]\Delta \dot{u}_{N1} \\ \Delta \dot{x}_{N2} &= [A_{N2}]\Delta x_{N2} + [D_{N2}]\Delta x_{N1} + [C_{N1}]\Delta u_{N1} + [C_{N2}]\Delta \dot{u}_{N1}\end{aligned}$$



$$\begin{aligned}
\Delta u_{N1} &= \Delta y_G \\
\Delta \dot{u}_{N1} &= \Delta \dot{y}_G \\
\text{where } \Delta y_G &= [C_G] \Delta x_G \\
\Delta \dot{y}_G &= [C_G] \Delta \dot{x}_G \\
\Delta u_{N1} &= [C_G] \Delta x_G \\
\Delta \dot{u}_{N1} &= [C_G] \Delta \dot{x}_G
\end{aligned}$$

$$\begin{aligned}
\Delta \dot{x}_{N1} &= [A_{N1}] \Delta x_{N1} + [D_{N1}] \Delta x_{N2} + [B_{N1}] [C_G] \Delta x_G + [B_{N2}] [C_G] [L \Delta x_G + [B_G] [H] \Delta x_{N1}] \\
\Delta \dot{x}_{N2} &= [A_{N2}] \Delta x_{N2} + [D_{N2}] \Delta x_{N1} + [C_{N1}] [C_G] \Delta x_G + [C_{N2}] [C_G] [L \Delta x_G + [B_G] [H] \Delta x_{N1}] \\
\Delta \dot{x}_{N1} &= [A_{N1}] \Delta x_{N1} + [D_{N1}] \Delta x_{N2} + [B_{N1}] [C_G] \Delta x_G + [B_{N2}] [C_G] L \Delta x_G + [B_{N2}] [C_G] [B_G] [H] \Delta x_{N1} \\
\Delta \dot{x}_{N2} &= [A_{N2}] \Delta x_{N2} + [D_{N2}] \Delta x_{N1} + [C_{N1}] [C_G] \Delta x_G + [C_{N2}] [C_G] L \Delta x_G + [C_{N2}] [C_G] [B_G] [H] \Delta x_{N1} \\
\Delta \dot{x}_G &= \left[ [A_G] + [B_G] [H] \left[ F [C_G] + \frac{x_L}{w_b} [C_G A_G] \right] \right] \Delta x_G + [B_G] [H] \Delta x_{N1} \\
\Delta \dot{x}_{N1} &= [[B_{N1}] [C_G] + [B_{N2}] [C_G] L] \Delta x_G + [[A_{N1}] + [B_{N2}] [C_G] [B_G] [H]] \Delta x_{N1} + [D_{N1}] \Delta x_{N2} \\
\Delta \dot{x}_{N2} &= [[C_{N1}] [C_G] + [C_{N2}] [C_G] L] \Delta x_G + [[D_{N2}] + [C_{N2}] [C_G] [B_G] [H]] \Delta x_{N1} + [A_{N2}] \Delta x_{N2}
\end{aligned}$$

Now the combined state model of generator and network is

$$\begin{bmatrix} \Delta \dot{x}_G \\ \Delta \dot{x}_{N1} \\ \Delta \dot{x}_{N2} \end{bmatrix} = \begin{bmatrix} \left[ [A_G] + [B_G] [H] \left[ F [C_G] + \frac{x_L}{w_b} [C_G A_G] \right] \right] & [B_G] [H] & [0] \\ [B_{N1}] [C_G] + [B_{N2}] [C_G] L & [[A_{N1}] + [B_{N2}] [C_G] [B_G] [H]] & [D_{N1}] \\ [C_{N1}] [C_G] + [C_{N2}] [C_G] L & [[D_{N2}] + [C_{N2}] [C_G] [B_G] [H]] & [A_{N2}] \end{bmatrix} \begin{bmatrix} \Delta x_G \\ \Delta x_{N1} \\ \Delta x_{N2} \end{bmatrix}$$

Now the final system equations can be written as

$$\Delta \dot{x}_T = [A_T] \Delta x_T$$

$$\text{where } x_T^t = [x_G^t \quad x_{N1}^t \quad x_{N2}^t]$$

### 4.1 Introduction

The IEEE working group on Subsynchronous Resonance has introduced one benchmark model for time-domain simulation of turbogenerator torsional oscillations [1]. Here Eigen value analysis approach is taken for investigation of small signal torsional oscillations. The results of this analysis is presented in 4.2 in 2 parts as 4.2.1, in which results were taken with fixed capacitor as the series compensating device and 4.2.2, in which results were taken with TCSC. the series compensating device. The PSCAD/EMTDC simulation results are given in 4.3.1 with capacitor and in 4.3.2 with a TCSC.

### 4.2 Eigen value analysis for SSR

#### 4.2.1 With fixed capacitor

Some of the critical eigen values of the complete system with series capacitor as the compensating device are listed in Table 4.1 for a series compensation level of  $X_c = 0.39$ . For this level, a steady-state operating point is chosen in which the machine operates with a power factor of 0.9 while delivering a power of 0.7 per unit. The infinite system voltage is 478 kV. With capacitor as the series device, real part of the eigenvalues corresponding to various torsional modal frequencies vary in magnitude and becomes unstable as the line series compensation changes. As the level of compensation increases, the oscillation frequency of the subsynchronous electrical mode decreases. In fact it can be seen that this mode approaches one of the torsional modes for various compensation levels. It is well known that SSR manifests when frequency of the electrical mode nears or coincides with one of the torsional modes. At the particular compensation level given in table 4.1 modes 5,4,3,2,1 are

unstable. It is also interesting to note that at compensation levels that cause SSR, the subsynchronous electrical mode has increased damping.

Table 4.1 Eigenvalues of the capacitor compensated system for compensation level of  $X_C = 0.39$

Modes	
Super sync.	$-4.43 \pm j625.5$
Sub sync.	$-3.84 \pm j141.6$
Mode 0	$-1.22 \pm j10.21$
Mode 1	$0.10 \pm j99.98$
Mode 2	$0.57 \pm j127.10$
Mode 3	$0.02 \pm j160.38$
Mode 4	$0 \pm j202.81$
Mode 5	$0 \pm j 298.18$

#### 4.2.2 With TCSC

The TCSC parameters are adjusted in such way that with the nominal operating point (at 76deg) the compensation level 50%. The parameters of the TCSC are given in Table A.3 in appendix A. As seen from Table 4.3, all the eigenvalues are having negative real parts. The controller parameter selected are  $K_p = -0.008$  and  $K_i = 0.17$ . Table 4.4 shows the eigenvalues of the complete system with  $K = -0.1$  and  $K_i = 0.3$ . Some of the torsional modes unstable in this case. The dampings of the electrical modes are less compared to a capacitor compensated system.

Table 4.2 Critical Modes of TCSC compensated system for compensation level of  $X_{TCSC} = 0.37$

Modes	
Super sync.	$-8.0 \pm j477.7$
Sub sync.	$-5.13 \pm j276.3$
Mode 0	$-1.22 \pm j9.8$
Mode 1	$-0.19 \pm j98.406$
Mode 2	$-0.57 \pm j127.10$
Mode 3	$-0.17 \pm j160.44$
Mode 4	$-0.05 \pm j202.75$
Mode 5	$-0.18 \pm j298.18$

### 4.3 PSCAD/EMTDC results for SSR

#### 4.3.1 with fixed Capacitor as series compensator

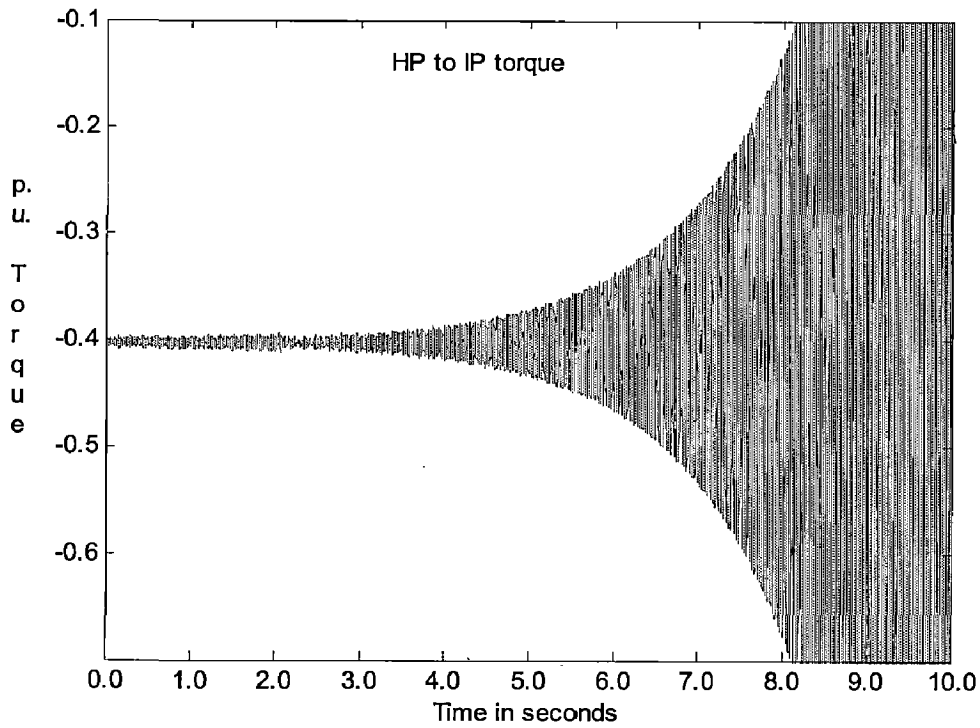


Fig.4.3.1.1 HP to IP torque

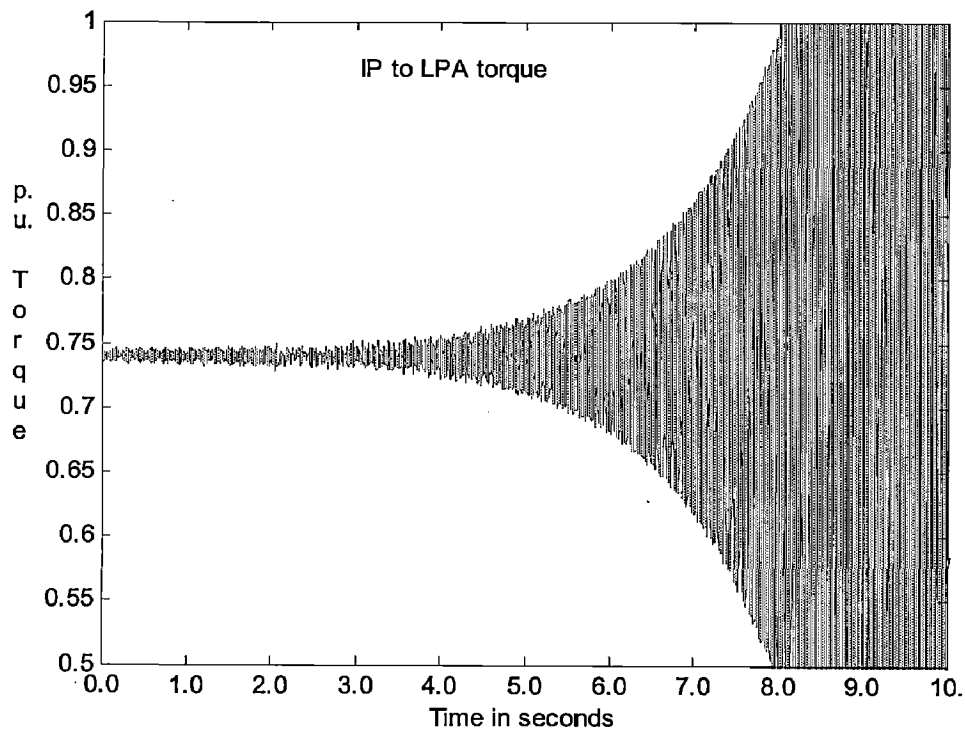


Fig.4.3.1.2 IP to LPA torque

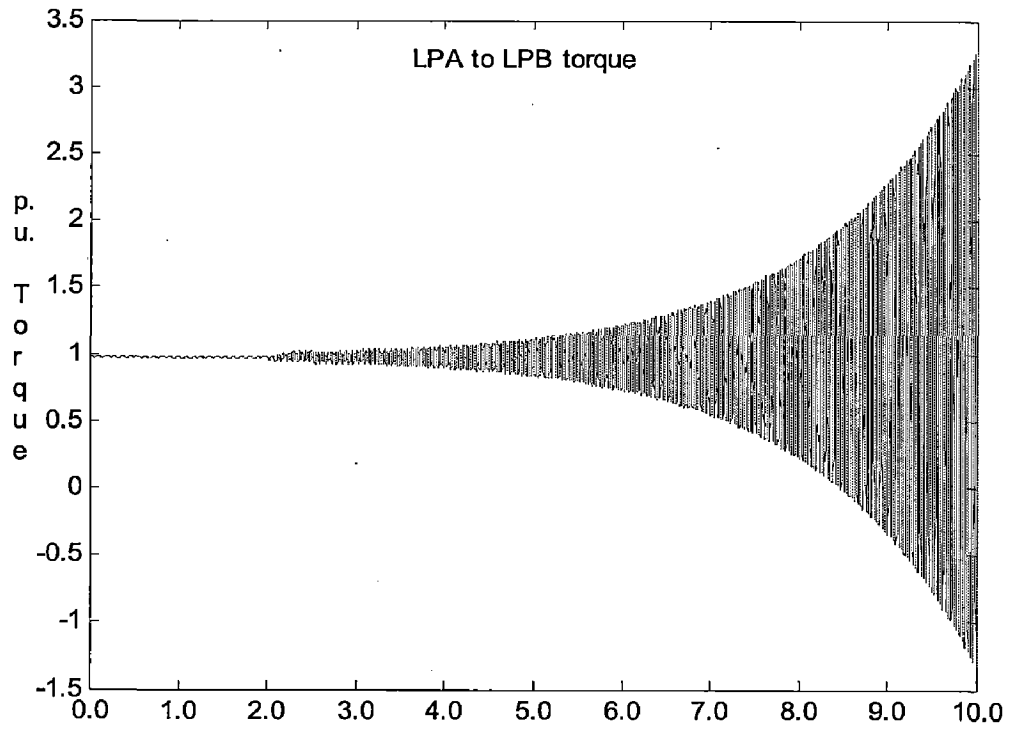


Fig 4.3.1.3 LPA to LPB Torque

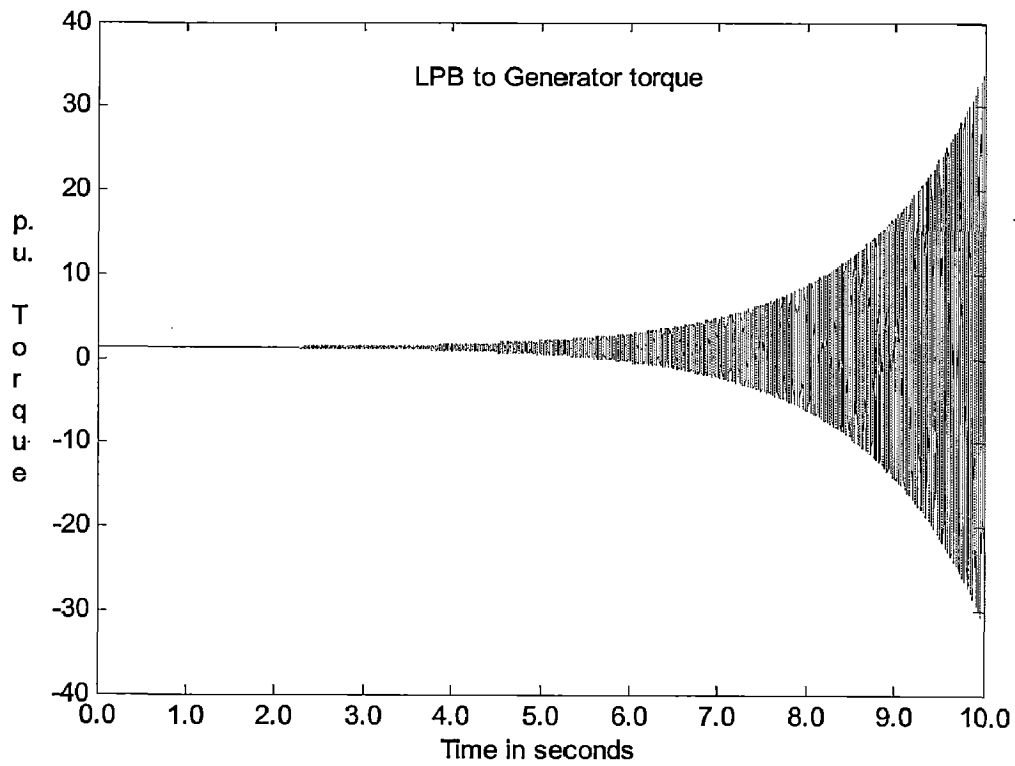


Fig. 4.3.1.4 LPB to Generator torque

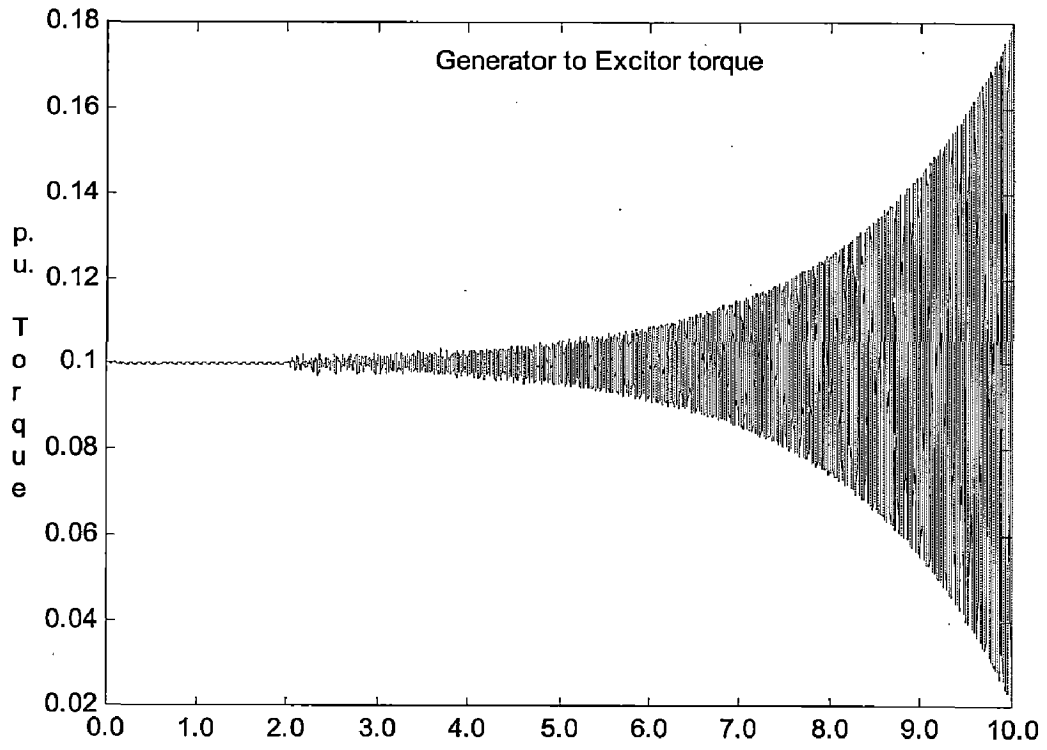


Fig 4.3.1.5 Genarator to Excitor torque

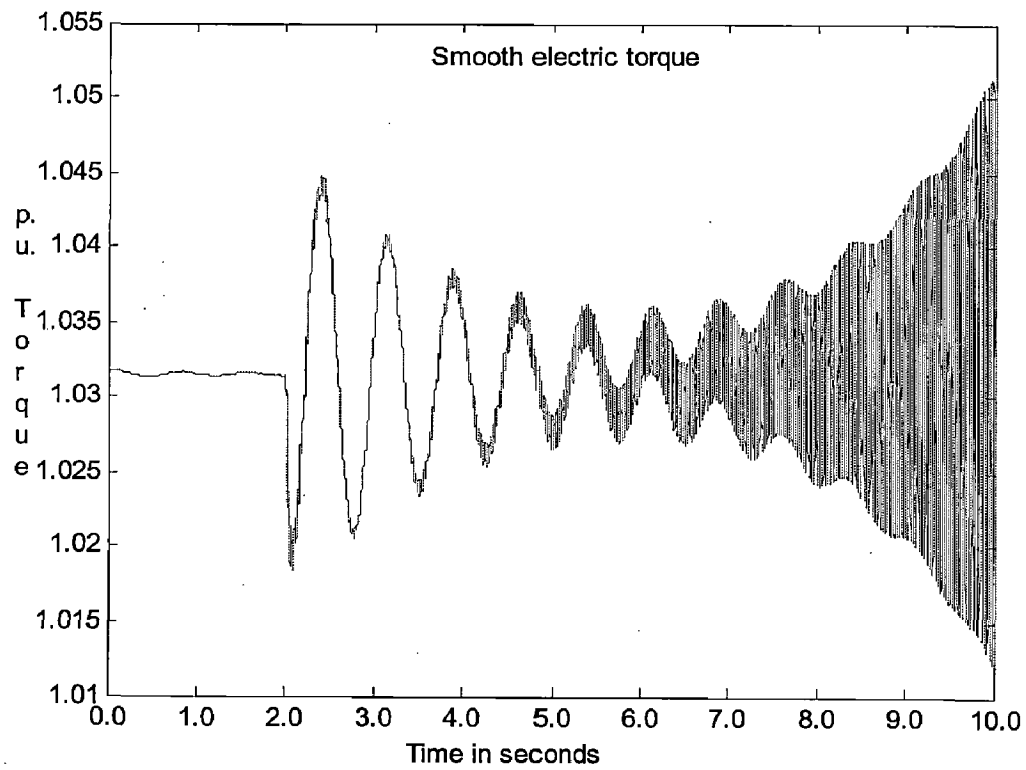


Fig 4.3.1.6 Smooth Electric torque

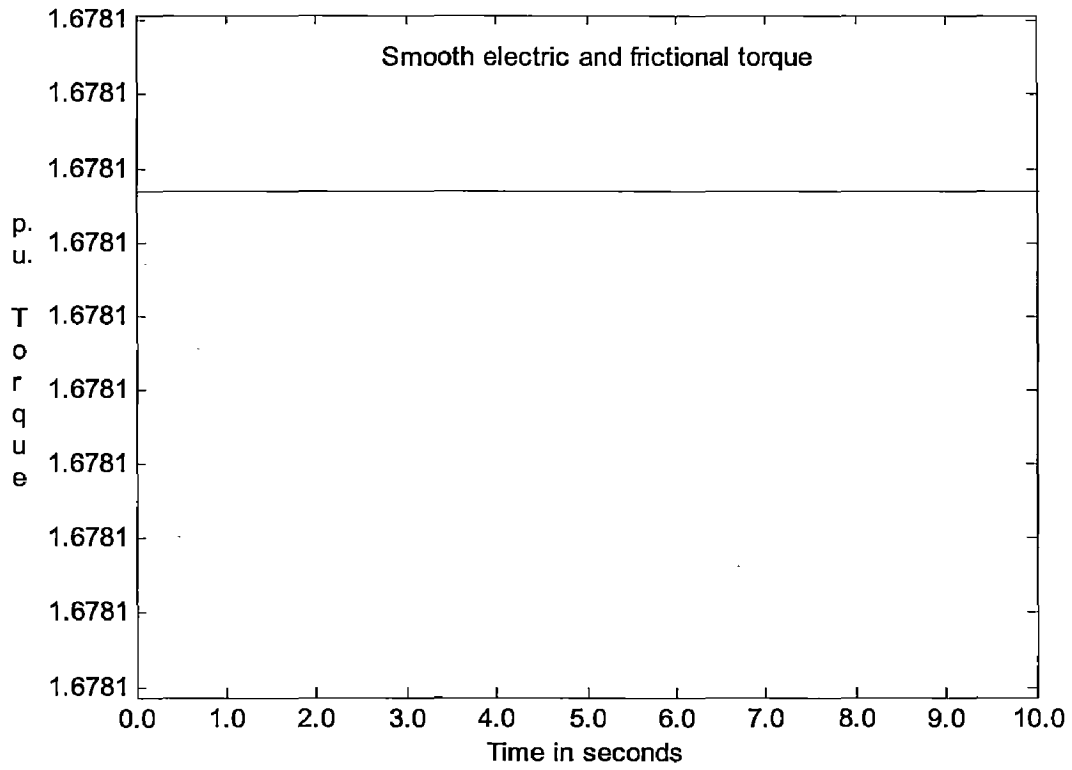


Fig 4.3.1.7 Smooth Electric and frictional torque

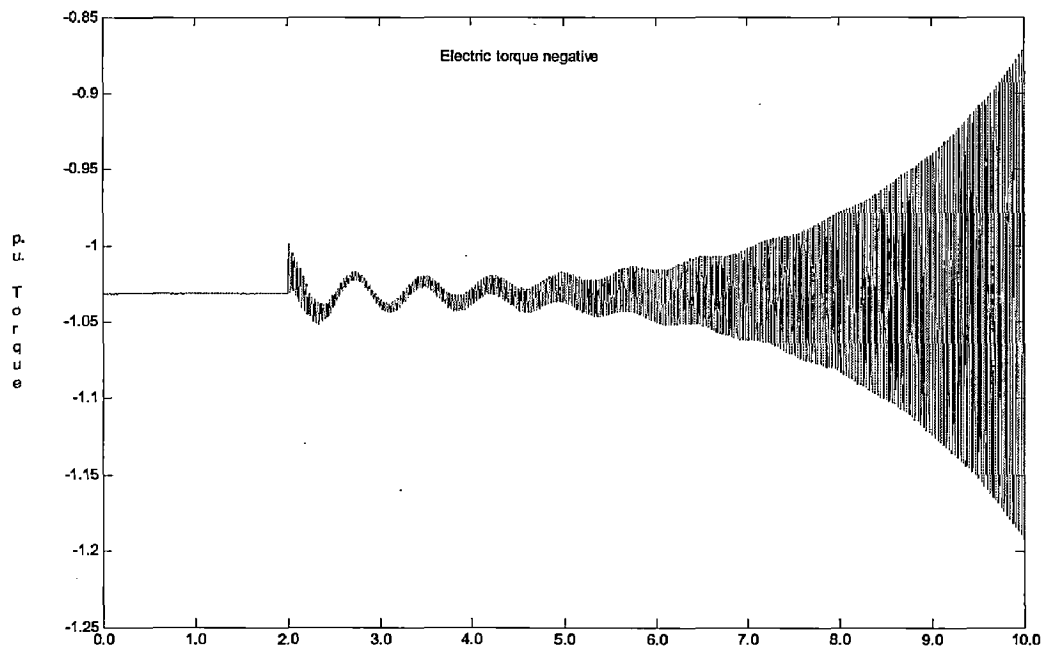


Fig 4.3.1.8 Electric torque negative



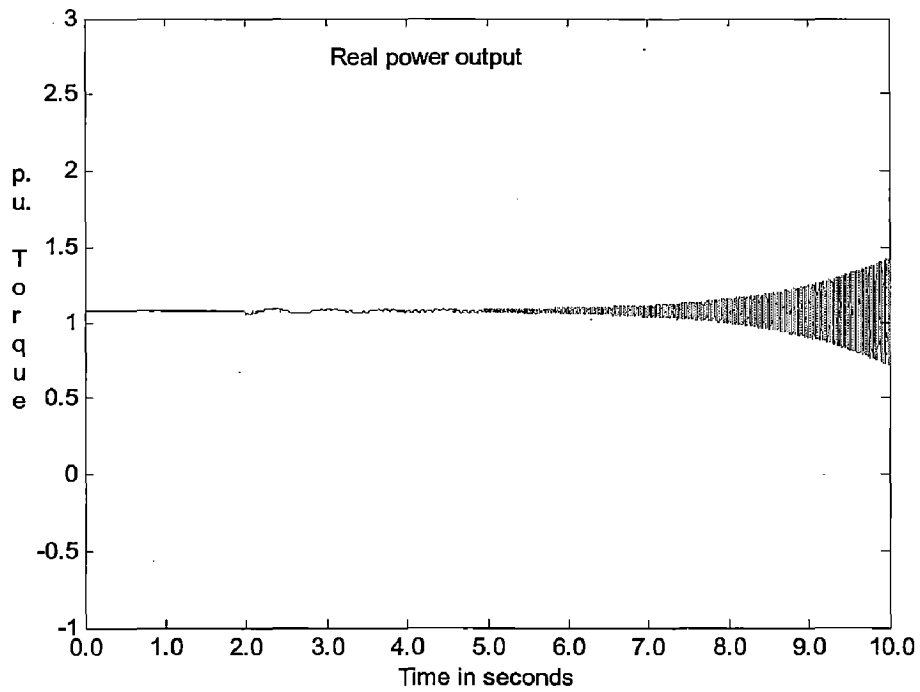


Fig 4.3.1.9 Real power output

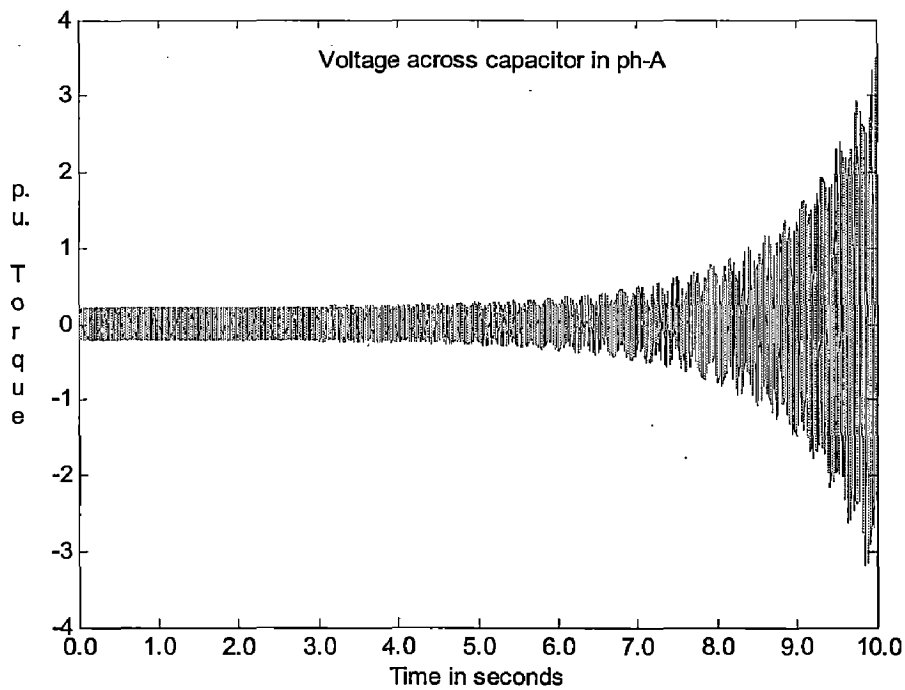


Fig.4.3.1.10 Voltage across capacitor in ph-A

The results obtained above are obtained by changing the compensation level i.e., by changing the voltage across the capacitor done by changing the value of capacitor.

4.3.2 with TCSC as series compensator

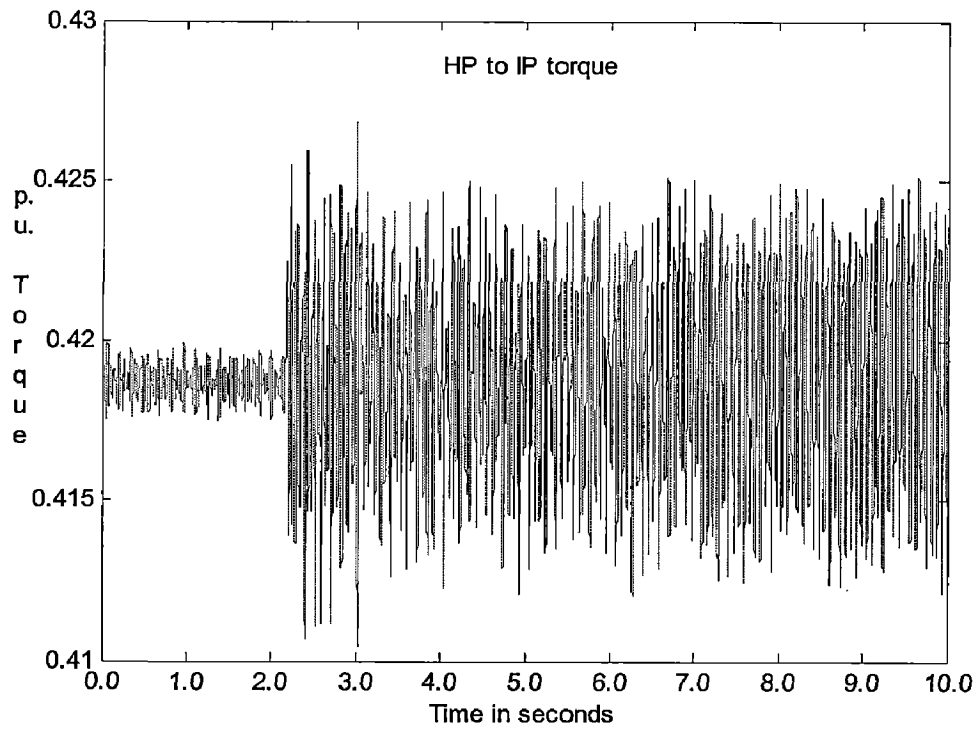


Fig 4.3.2.1 HP to IP torque

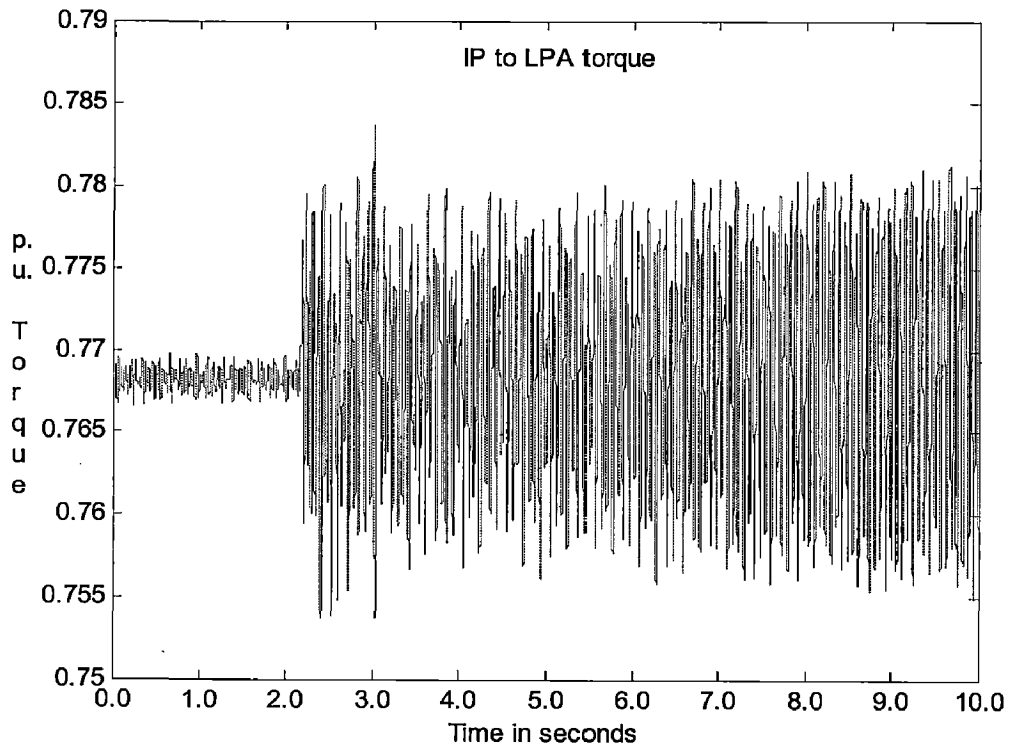


Fig 4.3.2.2 IP to LPA torque

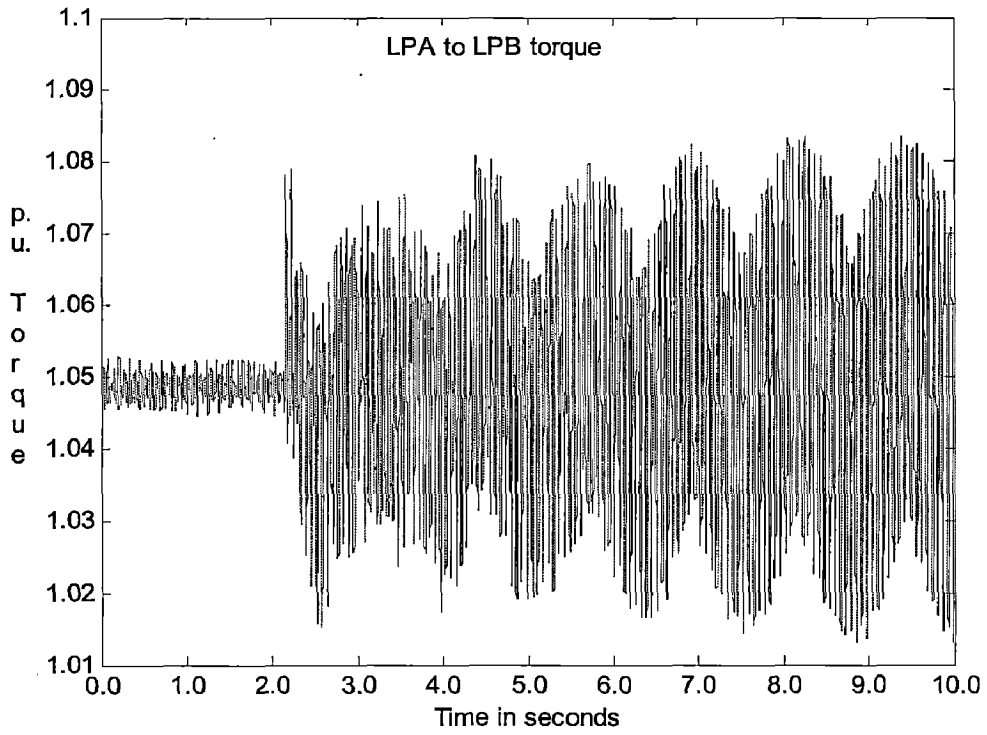


Fig. 4.3.2.3 LPA to LPB torque

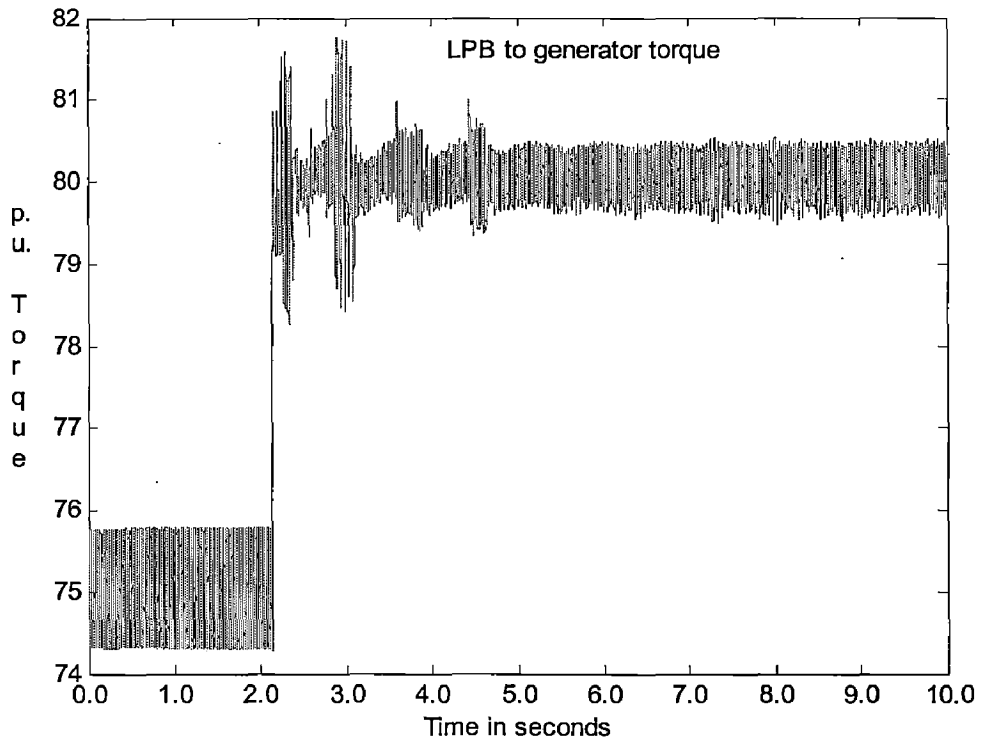


Fig 4.3.2.4 LPB to generator torque

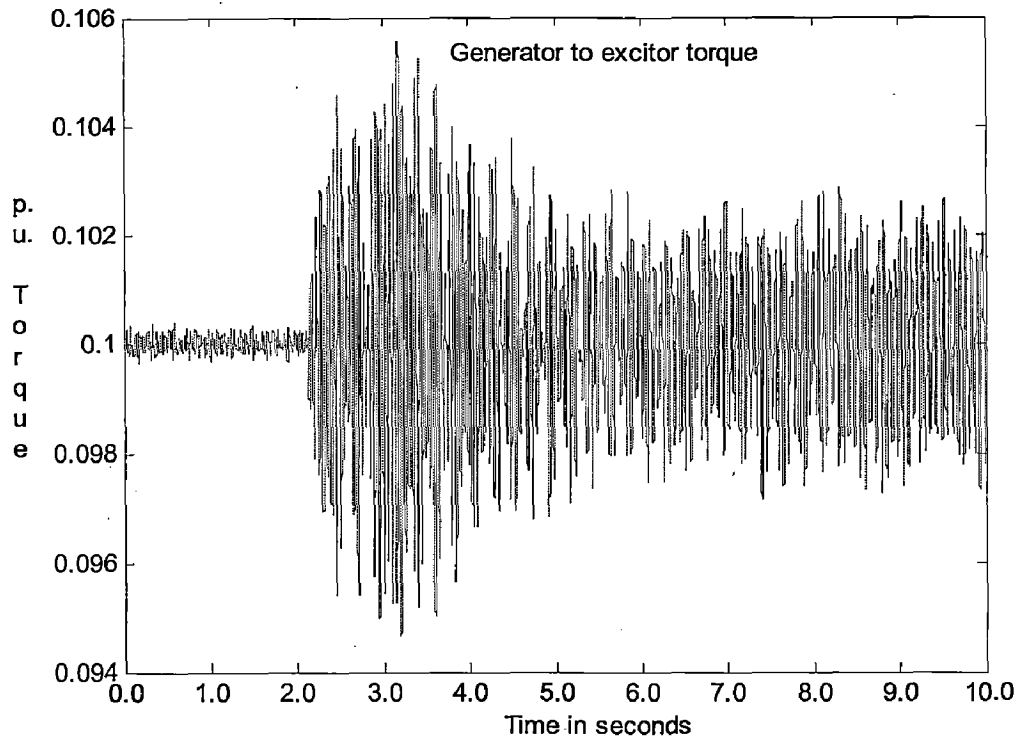


Fig 4.3.2.5 Generator to Excitor torque

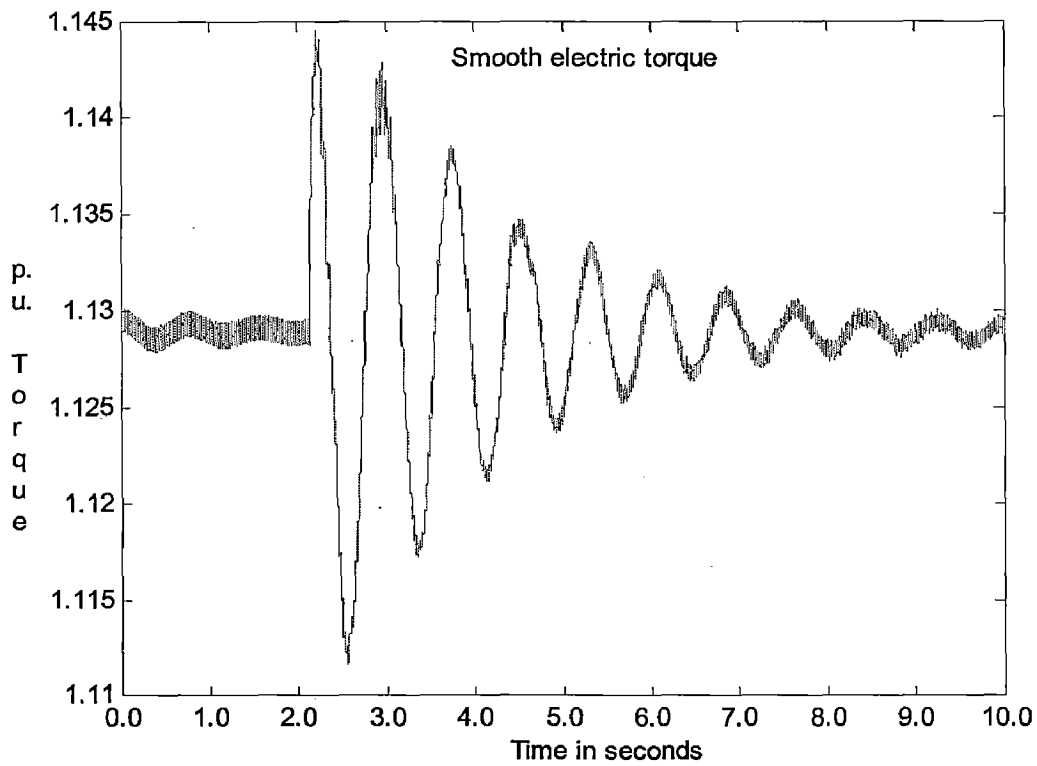


Fig 4.3.2.6 Smooth Electric torque

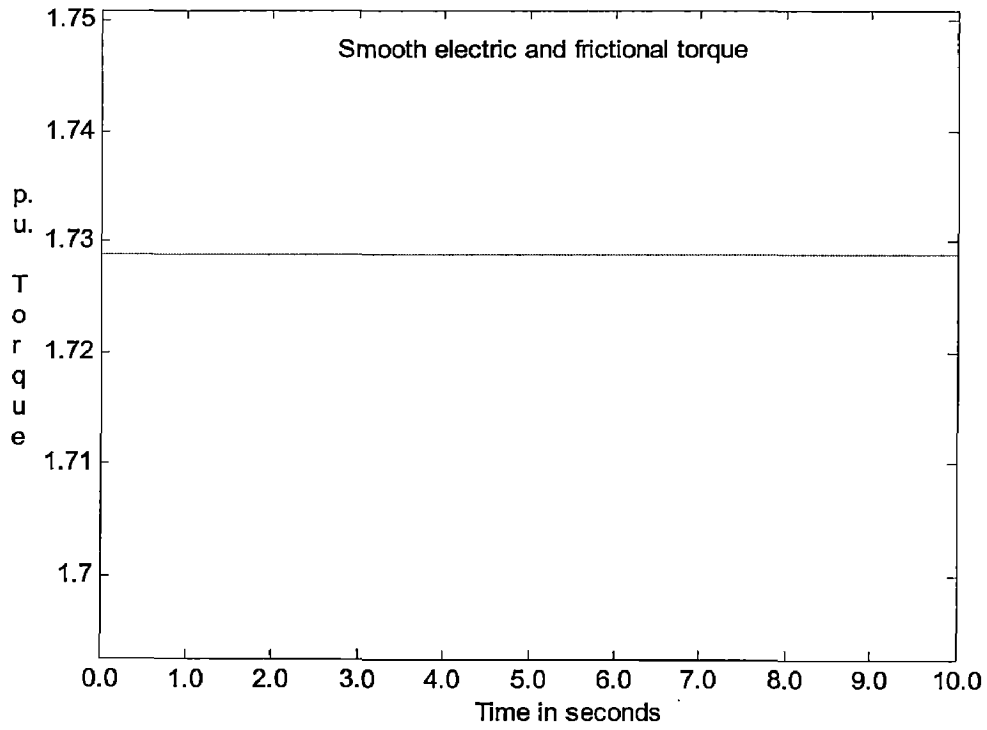


Fig. 4.3.2.7 Smooth electric and frictional torque

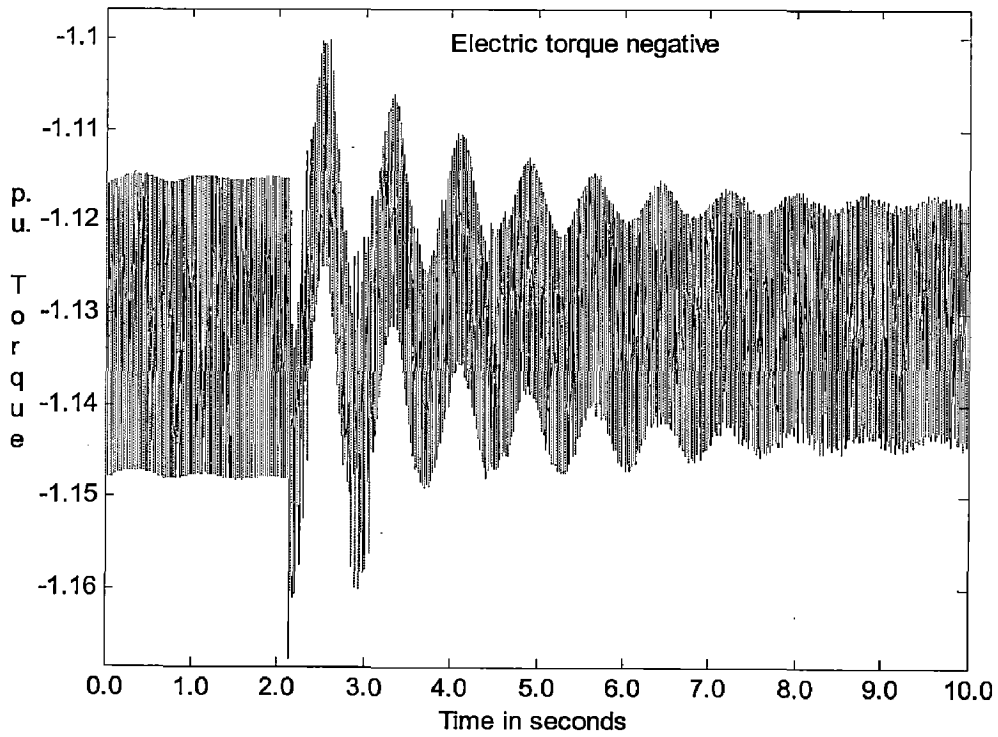


Fig 4.3.2.8 Electric torque negative

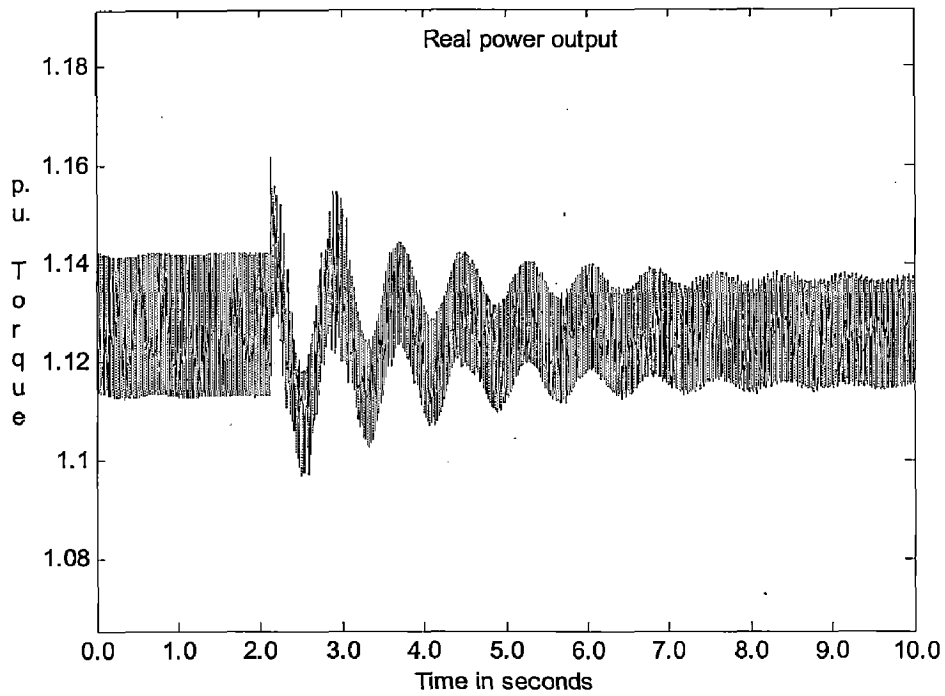


Fig.4.3.2.9 Real power output

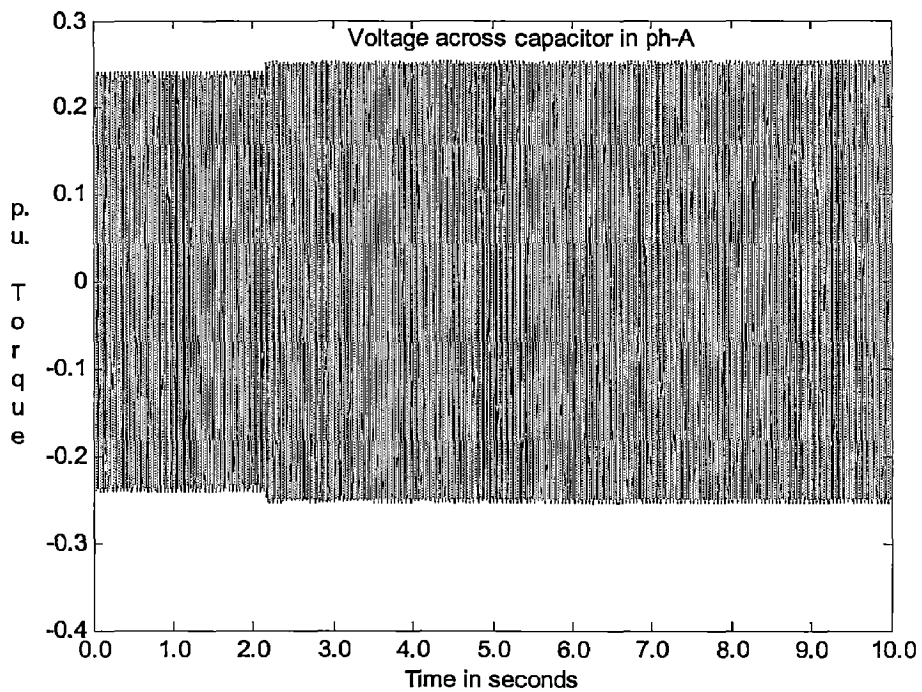


Fig.4.3.2.10 Voltage across capacitor in ph-A

The results obtained above are by changing the compensation level i.e., by changing the voltage across the capacitor done by changing the reference voltage.

This dissertation report presents a systematic study of small signal torsional characteristics of a TCSC compensated power system. IEEE first benchmark model is selected as the test system for the studies. A new model of TCSC is used in the study which includes the complete model of the controller and also model of the PLL is included in the modeling of the controller. The voltage across TCSC is taken as the feedback signal of the controller. The eigenvalue analysis shows that with suitable values of the PI controller and controlling the parameters of a PLL, a TCSC can damp the torsional oscillations in a series compensated power system. The results are compared with PSCAD/EMTDC simulation results.

IT'S CONTROLLER'S DATATable A.1 Electrical Parameters of the test system

Parameters	Values	Parameters	Values
R	0.02 ohm	$x_d'$	0.169
$X_T$	0.14	$T_{d0}'$	4.3
$X_L$	0.5	$x_q$	1.71
$X_{sys}$	0.06	$x_q'$	0.228
		$T_{q0}'$	0.85

Table A.2 Parameters of the turbine shaft system

Mass	Inertia constant(H)	Shaft section	Spring constant
HP	0.092897	HP-IP	19.303
IP	0.155589	IP-LPA	34.929
LPA	0.855867	LPA-LPB	52.038
LPB	0.884215	LPB-GEN	70.858
GEN	0.868495	GEN-EXC	2.822
EXC	0.0342165		



Table A.3 TCSC and TCSC controller data.

TCSC data (at nominal point)	
$c$	$42 \mu F$
$I_{TCR}$	$0.043 H$
$Fir. angle \alpha$	$78^\circ$
TCSC Controller data	
$k_p$	$-0.008 rad/kV$
$K_I$	$-0.17 rad/(kVs)$
$T_{d1}$	$1/220s$
$T_{d2}$	$1/1400s$
PLL $k_p$	20
$T_1$	$0.03 s$
$T_2$	$0.0095 s$

The stator and rotor flux linkages are given by

$$\Psi_d = x_d i_d + x_{ad} i_f \quad (\text{B.1})$$

$$\Psi_f = x_{ad} i_d + x_f i_f \quad (\text{B.2})$$

$$\Psi_q = x_q i_q + x_{aq} i_g \quad (\text{B.3})$$

$$\Psi_g = x_{aq} i_q + x_g i_g \quad (\text{B.4})$$

Solving B.2 and B.4

$$i_f = \frac{\Psi_f}{x_f} - \frac{x_{ad}}{x_f} i_d \quad (\text{B.5})$$

$$i_g = \frac{\Psi_g}{x_g} - \frac{x_{aq}}{x_g} i_q \quad (\text{B.6})$$

Substituting Eq.B.5 and B.6 in B.1 and B.3 respectively, we get

$$\Psi_d = x_d' i_d + E_q' \quad (\text{B.7})$$

$$\Psi_q = x_q' i_q + E_d' \quad (\text{B.8})$$

where

$$x_d' = x_d - \frac{x_{ad}^2}{x_f} \quad (\text{B.9})$$

$$x_q' = x_q - \frac{x_{aq}^2}{x_g} \quad (\text{B.10})$$

$$E_q' = \frac{x_{ad} \Psi_f}{x_f} \quad (\text{B.11})$$

$$E_d' = \frac{-x_{aq} \Psi_g}{x_g} \quad (\text{B.12})$$

The voltage equations for rotor are

$$\frac{1}{\omega_b} \frac{d\psi_f}{dt} = -R_f i_f + v_f \quad (\text{B.13})$$

$$\frac{1}{\omega_b} \frac{d\psi_g}{dt} = -R_g i_g \quad (\text{B.14})$$

Substituting B.5 and B.11 in B.13, we get

$$\frac{1}{\omega_b} \frac{x_f}{x_{ad}} \frac{dE_q'}{dt} = -\frac{R_f E_q'}{x_{ad}} + \frac{R_f x_{ad}}{x_f} i_d + v_f \quad (\text{B.15})$$

$$\frac{dE_q'}{dt} = \frac{\omega_b R_f}{x_f} \left[ -E_q' + \frac{x_{ad}^2}{x_f} i_d + \frac{x_{ad}}{R_f} v_f \right] \quad (\text{B.16})$$

$$= \frac{1}{T_{d0}'} \left[ -E_q' + (x_d - x_d') i_d + E_{fd} \right] \quad (\text{B.17})$$

where

$$E_{fd} = \frac{x_{ad}}{R_f} v_f \quad (\text{B.18})$$

$$T_{d0}' = \frac{x_f}{\omega_b R_f} \quad (\text{B.19})$$

Now considering the stator equations

$$E_q' + x_d' i_d' - R_a i_q = v_q \quad (\text{B.20})$$

$$E_d' - x_q' i_q' - R_a i_d = v_d \quad (\text{B.21})$$

If transient saliency is neglected by letting

$$x_d' = x_q' = x' \quad (\text{B.22})$$

We can combine B.20 and B.21 into a single complex equation given by

$$(E_q' + jE_d') - (R_a + jx')(i_q + ji_d) = v_q + jv_d \quad (\text{B.23})$$

The above equation represents an equivalent circuit of the stator shown in fig.6.2

(a). This shows a voltage source  $(E_q' + jE_d')$  behind equivalent impedance  $(R_a + jx')$ .

The variables (D-Q) in Kron's frame of reference are related to the variables (d-q) in Park's frame of reference by

$$(f_Q + jf_D) = (f_q + jf_d)e^{j\delta} \tag{B.24}$$

where  $f$  can represent voltage or current. Applying B.24 to B.23, we get

$$(E_Q' + jE_D') - (R_a + jx')(i_Q + ji_D) = v_Q + jv_D \tag{B.25}$$

B.25 also represents an equivalent circuit of the stator shown in fig.6.2.

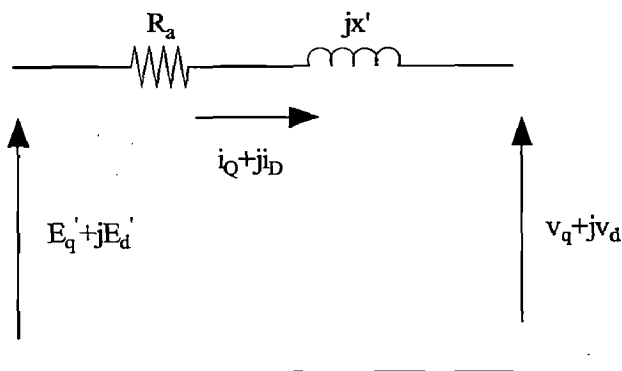


Fig.6.2(a)

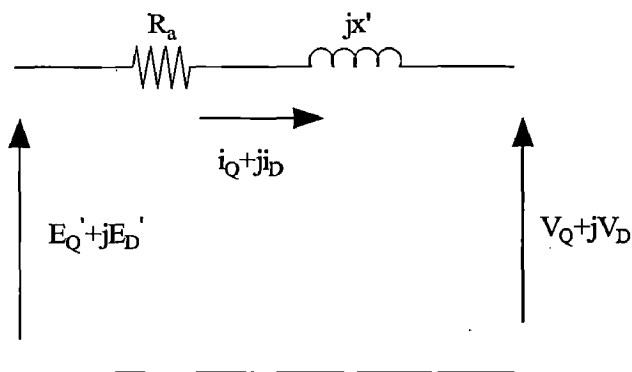


Fig 6.2(b)

Fig.6.2 Stator equivalent circuits

It is assumed that the external network connecting the generator terminals to the infinite bus is linear two ports. Whatever may be the configuration of the external network, it can be represented by the two port network parameters. As only the first

port, connected to the generator terminals is of interest, the voltage there can be expressed as

$$\hat{V}_t = \frac{\hat{I}_a}{y_{11}} + h_{12}\hat{E}_b \quad (\text{B.26})$$

Where  $y_{11}$  is the short circuit self admittance of the network, measured at the generator terminals,  $h_{12}$  is open circuit voltage gain. For a simple network consisting of only series impedance ( $R_e + jX_e$ ), it is not difficult to see that

$$\frac{1}{y_{11}} = R_e + jx_e \quad (\text{B.27})$$

In general case, let

$$\frac{1}{y_{11}} = z_R + jz_I, h_{12} = h_1 + jh_2 \quad (\text{B.28})$$

Eq.B.26 can be expressed as

$$(v_q + jv_d)e^{j\delta} = (z_R + jz_I)(i_q + ji_d)e^{j\delta} + (h_1 + jh_2)E_b \quad (\text{B.29})$$

Multiplying both sides by  $e^{-j\delta}$ , we get

$$(v_q + jv_d) = (z_R + jz_I)(i_q + ji_d) + (h_1 + jh_2)E_b e^{-j\delta} \quad (\text{B.30})$$

Equating real and imaginary parts, we get

$$v_q = z_R i_q - z_I i_d + h_1 E_b \cos \delta + h_2 E_b \sin \delta \quad (\text{B.31})$$

$$v_d = z_I i_q + z_R i_d + h_2 E_b \cos \delta - h_1 E_b \sin \delta \quad (\text{B.32})$$

The simplest external network is a series impedance ( $R_e + jX_e$ ). If  $R_e = 0$ , then

$$z_R = 0, \quad z_I = x_e, \quad h_1 = 1.0, \quad h_2 = 0 \quad (\text{B.33})$$

Substituting these values in B.31 and B.32 we get

$$v_q = -x_e i_d + E_b \cos \delta \quad (\text{B.34})$$

$$v_d = x_e i_q - E_b \sin \delta \quad (\text{B.35})$$

If  $R_a = 0$ , the substitution of above equation in B.20 and B.21 gives

$$i_d = \frac{E_b \cos \delta - E_q'}{(x_e + x_d')} \quad (\text{B.36})$$

$$i_q = \frac{E_b \sin \delta + E_d'}{(x_e + x_q')} \quad (\text{B.37})$$

Equations B.36 and B.37 can be substituted in eq.B.17 to eliminate the non-state variables and express the equations in the form

$$\dot{x}_m = f_m(x_m, u_m) \quad (\text{B.38})$$

Where

$$x_m' = [\delta \quad S_m \quad E_q' \quad E_d']$$

$$u_m' = [E_{fd} \quad T_m]$$

The system equations B.38 are nonlinear and have to be solved numerically. In solving these equations it is to be assumed that the system is at a stable equilibrium point till time  $t=0$ , and a disturbance occurs at  $t=0$  or later. It is necessary to calculate the initial conditions  $x_0$  at time  $t=0$  based on the system operating point determined from load (power) flow.

From power flow calculations in steady state, we get the real and reactive power ( $P_t$  and  $Q_t$ ) the voltage magnitude ( $V_t$ ) and angle ( $\theta$ ) at the generator terminals. Here  $\theta$  is the angle w.r.to. infinite bus.

In the steady state, the derivative of all state variables,  $\dot{x} = 0$ . From this condition, we get

$$E_{q0}' = E_{fd0} + (x_d - x_d')\dot{i}_{d0} \quad (\text{B.39})$$

$$E_{d0}' = -(x_q - x_q')\dot{i}_{q0} \quad (\text{B.40})$$

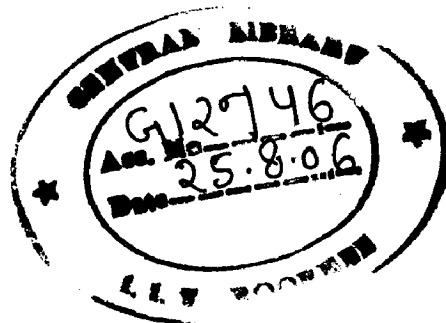
$$T_{m0} = T_{e0} = E_{q0}'i_{q0} + E_{d0}'i_{d0} + (x_d'x_q')\dot{i}_{d0}i_{q0} \quad (\text{B.41})$$

In the above equations, the subscript 0 indicates the operating values.

Substituting B.39 and B.40 in B.20 and B.21, we got

$$E_{fd0} + x_d i_{d0} - R_a i_{q0} = v_{q0} \quad (\text{B.42})$$

$$-x_q i_{q0} - R_a i_{d0} = v_{d0} \quad (\text{B.43})$$



From above one can obtain

$$E_{fd0} + (x_d - x_q)j_{d0} = (v_{q0} + jv_{d0}) + (R_a + jx_q)(i_{q0} + ji_{d0}) = V_t e^{-j\delta} - \delta + (R_a + jx_q)I_a e^{-j\delta} \quad (\text{B.44})$$

Defining

$$E_q \angle \delta = \hat{V}_t + (R_a + jx_q)\hat{I}_a \quad (\text{B.45})$$

We can express

$$E_{fd0} = E_{q0} - (x_d - x_q)j_{d0} \quad (\text{B.46})$$

Now the procedure for the computation for initial conditions is given below

1. Compute  $\hat{I}_{a0}$  from

$$\hat{I}_{a0} = I_{a0} \angle \phi_0 = \frac{P_{t0} - jQ_{t0}}{V_{t0} \angle -\theta_0}$$

2. Compute  $E_{q0}$  and  $\delta_0$  from

$$E_{q0} \angle \delta = V_{t0} \angle \theta_0 + (R_a + jx_q)I_{a0} \angle \phi_0$$

3. Compute

$$i_{d0} = -i_{a0} \sin(\delta_0 - \phi_0)$$

$$i_{q0} = i_{a0} \cos(\delta_0 - \phi_0)$$

$$v_{d0} = -V_{t0} \sin(\delta_0 - \theta_0)$$

$$v_{q0} = V_{t0} \cos(\delta_0 - \theta_0)$$

4. Compute

$$E_{fd0} = E_{q0} - (x_d - x_q)j_{d0}$$

$$E_{q0}' = E_{fd0} + (x_d - x_d')j_{d0}$$

$$E_{d0}' = -(x_q - x_q')j_{q0}$$

The generator terminal voltage angle  $\theta_0$  can be obtained from

$$P_t = \frac{V_{t0} E_b \sin \theta_0}{R + jx_e}$$

$$I_a = \frac{V_t - E_b \angle 0}{R + jx_e}$$

$$E_{q0} = V_{t0} \angle \theta_0 + jx_q I_a$$

$$\text{magnitude\_of\_}E_{q0} = \text{abs}(E_{q0})$$

$$\text{delta} = \text{angle}(E_{q0})$$

$$I_{d0} = -I_a \sin(\text{delta} - \text{theta0})$$

$$I_{q0} = I_a \cos(\text{delta} - \text{theta0})$$

$$E_{fd0} = E_{q0} - (x_d - x_q) i_{d0}$$

$$E_{q0\_dash} = E_{fd0} + (x_d - x_{d\_dash}) i_{d0}$$

$$E_{d0\_dash} = -(x_q - x_{q\_dash}) i_{q0}$$

$$F_{iD0} = X_{d\_dash} * I_{d0} + E_{q0\_dash}$$

$$F_{iQ0} = X_{q\_dash} * I_{q0} - E_{d0\_dash}$$



---

**FROM  $abc$  TO  $DQ0$  COORDINATE**


---

A single phase  $\pi$  equivalent of a transmission line is shown in fig. C.1 .However it is to be noted that the co-efficient matrices, inductance  $[L]$ , resistance  $[R]$  and capacitance  $[C]$  are all  $3 \times 3$  matrices. These are defined as

$$[L] = \begin{bmatrix} L_s & L_m & L_m \\ L_m & L_s & L_m \\ L_m & L_m & L_s \end{bmatrix}, [R] = \begin{bmatrix} R_s & R_m & R_m \\ R_m & R_s & R_m \\ R_m & R_m & R_s \end{bmatrix}, [C] = \begin{bmatrix} C_s & C_m & C_m \\ C_m & C_s & C_m \\ C_m & C_m & C_s \end{bmatrix}$$

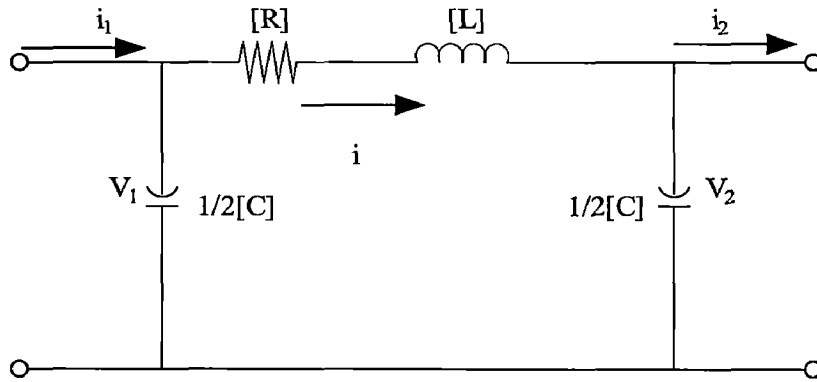


Fig.C.1 A single phase  $\pi$  equivalent of a transmission line

The network equations are

$$[L] \frac{di}{dt} + [R]i = v_1 - v_2 \quad (C.1)$$

$$\frac{1}{2}[C] \frac{dv_1}{dt} = i_1 - i \quad (C.2)$$

$$\frac{1}{2}[C] \frac{dv_2}{dt} = i_2 - i \quad (C.3)$$

where  $v_1, v_2, i_1, i_2$  are 3-dimensional vectors, with phase variables as elements. For example

$$i' = [i_a \quad i_b \quad i_c]$$

$$v_1' = [v_{1a} \quad v_{1b} \quad v_{1c}]$$

$$v_2' = [v_{2a} \quad v_{2b} \quad v_{2c}]$$

If generator is described by variables in d-q components, using Park's transformation, it stands to reason that the external network equations should also be expressed in d-q components. However, there is one problem and that is Park's transformation is not unique and each generator has individual d-q components (corresponding to the individual transformation).

For a connected network, it is obvious that the entire network is to be transformed using a single transformation with reference to a common, synchronously rotating reference frame. Such transformation is termed as Kron's transformation defined as

$$\begin{bmatrix} f_a \\ f_b \\ f_c \end{bmatrix} = \sqrt{\frac{2}{3}} \begin{bmatrix} \cos \theta_0 & \sin \theta_0 & \frac{1}{\sqrt{2}} \\ \cos\left(\theta_0 - \frac{2\pi}{3}\right) & \sin\left(\theta_0 - \frac{2\pi}{3}\right) & \frac{1}{\sqrt{2}} \\ \cos\left(\theta_0 + \frac{2\pi}{3}\right) & \sin\left(\theta_0 - \frac{2\pi}{3}\right) & \frac{1}{\sqrt{2}} \end{bmatrix} \begin{bmatrix} f_D \\ f_Q \\ f_0 \end{bmatrix} = [C_K] f_{DQ0}$$

$$\text{where } f_{DQ0} = \begin{bmatrix} f_D \\ f_Q \\ f_0 \end{bmatrix}$$

It is to be noted that f can be any variable, voltage or current.  $\theta_0$  is defined as

$$\theta_0 = \omega_0 t + \gamma$$

where  $\omega_0$  is the average (synchronous frequency) in the network in the steady state and  $\gamma$  is constant. There is no loss of generality if  $\gamma$  is assumed to be zero. The difference between Kron's and Park's transformation lies in  $\theta_0$  being replaced by  $\theta$  in Park's transformation.  $\theta$  is defined by

$$\theta = \omega_0 t + \delta$$

It is to be noted that  $\delta$  is dependent on the generator and not a common variable.  $[C_K]$  is defined such that

$$[C_K]^{-1} = [C_K]^t$$

In other words,  $[C_K]$  is an orthogonal matrix and satisfies the condition for a power invariant transformation.

The relationship between  $[C_P]$  and  $[C_K]$  is given by

$$[C_P] = [C_K][T_1]$$

$$\text{where } [T_1] = \begin{bmatrix} \cos \delta & \sin \delta & 0 \\ -\sin \delta & \cos \delta & 0 \\ 0 & 0 & 1 \end{bmatrix}$$

It is to be noted that  $[T_1]$  is also an orthogonal matrix. Actually,  $[T_1]$  defines the transformation between Park's and Kron's variables, as

$$\begin{bmatrix} f_D \\ f_Q \\ f_0 \end{bmatrix} = [T_1] \begin{bmatrix} f_d \\ f_q \\ f_0 \end{bmatrix}$$

where  $f_d, f_q$  are Park's components and  $f_D, f_Q$  are Kron's components (with respect to) a synchronously rotating reference frame). Note that subscripts D, Q are associated with Kron's transformation. This convention will be followed throughout.

Apply Kron's transformation to C.1, C.2, C.3 results in (expressing only positive and negative sequence)

$$L_1 \frac{di_D}{dt} + \omega_0 L_1 i_Q + R_1 i_D = v_{1D} - v_{2D}$$

$$L_2 \frac{di_Q}{dt} - \omega_0 L_1 i_D + R_1 i_Q = v_{1Q} - v_{2Q}$$

$$\frac{1}{2} C_1 \frac{dv_{1D}}{dt} + \frac{\omega_0}{2} C_1 v_{1Q} = i_{1D} - i_D$$

$$\frac{1}{2} C_1 \frac{dv_{1Q}}{dt} - \frac{\omega_0}{2} C_1 v_{1D} = i_{1Q} - i_Q$$

$$\frac{1}{2} C_1 \frac{dv_{2D}}{dt} + \frac{\omega_0}{2} C_1 v_{2Q} = i_D - i_{2D}$$

$$\frac{1}{2} C_1 \frac{dv_{2Q}}{dt} - \frac{\omega_0}{2} C_1 v_{2D} = i_Q - i_{2Q}$$

The non-zero elements of  $[A_e]$  are given by

$$A_e(1,1) = \frac{-R_a * \omega_b}{x_d'}$$

$$A_e(1,2) = -\omega_b$$

$$A_e(1,4) = \frac{R_a * \omega_b}{x_d'}$$

$$A_e(2,1) = \omega_b$$

$$A_e(2,2) = -\frac{R_a * \omega_b}{x_q'}$$

$$A_e(2,3) = -\frac{R_a * \omega_b}{x_q'}$$

$$A_e(3,2) = -\frac{1}{T_{q0}'} * \left( \frac{X_q}{X_q'} - 1 \right)$$

$$A_e(3,3) = -\frac{X_q}{T_{q0}' * X_q'}$$

$$A_e(4,1) = -\frac{1}{T_{d0}'} * \left( \frac{X_d}{X_d'} - 1 \right)$$

$$A_e(4,4) = -\frac{X_d}{T_{d0}' * X_d'}$$

The non-zero elements of  $[B_{e1}]$  are functions of  $\delta$  given by

$$B_{e1}(1,1) = -\omega_b * \cos \delta$$

$$B_{e1}(1,2) = -\omega_b * \sin \delta$$

$$B_{e1}(2,1) = -\omega_b * \sin \delta$$

$$B_{e1}(2,2) = -\omega_b * \cos \delta$$

The non-zero element of the column vector  $[B_{e2}]$  are

$$B_{e2} = \frac{1}{T_{d0}'}$$

Also the non-zero elements of  $[C_e]$  are functions of  $\delta$  given by

$$Ce(1,1) = -Ce(1,4) = \frac{\cos \delta}{x_d'}$$

$$Ce(1,2) = Ce(1,3) = \frac{\sin \delta}{x_q'}$$

$$Ce(2,1) = -Ce(2,4) = -\frac{\sin \delta}{x_d'}$$

$$Ce(2,2) = -Ce(2,3) = \frac{\cos \delta}{x_q'}$$

The non-zero elements of  $[B_{e3}]$  are

$$B_{e3}(1,1) = \omega_b * v_{qo}$$

$$B_{e3}(2,1) = \omega_b * v_{do}$$

$$B_{e3}(1,2) = \omega_b * \varphi_{qo}$$

$$B_{e3}(2,2) = \omega_b * \varphi_{do}$$

$$[C_{em}] = \left[ \frac{\Delta C_e}{\Delta \delta} \right] [x_{e0} \ 0],$$

Now the non-zero elements of  $[A_m]$  are

$$A_m(1, 4) = \omega_B$$

$$A_m(2, 2) = -D_{exc} / (2 * H_{exc});$$

$$A_m(2, 3) = 1 / (2 * H_{exc})$$

$$A_m(3, 2) = -K_{lge} * W_b$$

$$A_m(3, 4) = -K_{exc};$$

$$A_m(4, 4) = -D_m / (2 * H_m);$$

$$A_m(4, 5) = 1 / (2 * H_m);$$

$$A_m(5, 4) = K_{lbg}$$

$$A_m(5, 6) = -K_{lbg} * \omega_B$$

$$A_m(6, 6) = -D_{lpb} / (2 * H_{lpb})$$

$$A_m(6, 7) = -1/(2 * H_{lpa})$$

$$A_m(7, 6) = K_{lab} * \omega_b$$

$$A_m(7, 8) = -K_{lab} * \omega_b$$

$$A_m(8, 8) = -D_{lpa} / (2 * H_{lpa})$$

$$A_m(8, 9) = -1/(2 * H_{lpa})$$

$$A_m(9, 8) = K_{il} * \omega_b$$

$$A_m(9, 10) = -K_{il} * \omega_b$$

$$A_m(10, 10) = -D_{ip} / (2 * H_{ip})$$

$$A_m(10, 11) = -1/(2 * H_{ip})$$

$$A_m(11, 10) = -K_{ip} * \omega_b$$

$$A_m(11, 12) = -K_{ip} * \omega_b$$

$$A_m(12, 12) = -D_{hp} / (2 * H_{hp})$$

The column vector  $B'_{m1}$  is

$$[0 \ 0 \ 0 \ -\frac{1}{2H_m} \ 0 \ 0 \ 0 \ 0 \ 0 \ 0 \ 0 \ 0]$$

Where  $[C_{me}]$  a row vector is whose elements are

$$C_{me}(1) = \frac{(X_d' - X_q')}{X_d' * X_q'} \phi_{q0} + \frac{E_{d0}'}{X_q'}$$

$$C_{me}(2) = \frac{(X_d' - X_q')}{X_d' * X_q'} \phi_{d0} + \frac{E_{q0}'}{X_d'}$$

$$C_{me}(3) = \frac{\phi_{d0}}{X_q'}$$

$$C_{me}(4) = \frac{\phi_{q0}}{X_d'}$$

Where

$$A_{NI} = \begin{bmatrix} \frac{1}{T_f} & -\omega_b \\ \omega_b & \frac{1}{T_f} \end{bmatrix}$$

Where the non-zero components of the unknown coefficients are

$$D_{N1} = \text{zeros}(2, 11)$$

$$D_{N1}(1, 1) = \frac{1}{T_f} * \left(1 - \frac{\omega_d^2}{\omega_n^2}\right)$$

$$D_{N1}(1, 3) = \frac{1}{T_f} * \left(1 - \frac{\omega_d^2}{\omega_n^2}\right)$$

$$D_{N1}(2, 2) = \frac{1}{T_f} * \left(1 - \frac{\omega_d^2}{\omega_n^2}\right)$$

$$D_{N1}(2, 4) = \frac{1}{T_f} * \left(1 - \frac{\omega_d^2}{\omega_n^2}\right)$$

$$D_{N1}(1, 4) = \frac{1}{T_f} * \left(\frac{\zeta_d * \omega_d}{\omega_n^2} - \frac{\zeta_n}{\omega_n}\right)$$

$$D_{N1}(2, 6) = \frac{1}{T_f} * \left(\frac{\zeta_d * \omega_d}{\omega_n^2} - \frac{\zeta_n}{\omega_n}\right)$$

$$B_{N1} = \text{zeros}(2, 2)$$

$$B_{N2} = \text{zeros}(2, 2)$$

$$A_{N2} = \text{zeros}(11, 11)$$

$$A_{N2}(3, 5) = 1$$

$$A_{N2}(4, 6) = 1$$

$$A_{N2}(5, 1) = \omega_d^2$$

$$A_{N2}(6, 2) = \omega_d^2$$

$$A_{N2}(5, 3) = -\omega_d^2$$

$$A_{N2}(6, 4) = -\omega_d^2$$

$$A_{N_2} (5, 5) = -\omega_d * zetaD$$

$$A_{N_2} (6, 6) = -\omega_d * zetaD$$

$$A_{N_2} (7, 7) = -1/T_{d2}$$

$$A_{N_2} (8, 9) = K_{iplltc}$$

$$A_{N_2} (9, 8) = K_{isplltc}$$

$$A_{N_2} (9, 9) = -K_{isplltc}$$

$$A_{n2} (11, 7) = \frac{1}{T_{d1}}$$

$$A_{n2} (11, 8) = -\frac{1}{T_{d1}}$$

$$A_{n2} (11, 9) = -\frac{1}{T_{d1}}$$

$$A_{n2} (11, 10) = \frac{1}{T_{d1}}$$

$$A_{n2} (11, 11) = \frac{1}{T_{d1}}$$

$$D_{n2} = \text{zeros} (11, 2)$$

$$D_{n2} (7,1) = \frac{x_{4Q0}}{T_{d2} (x_{4D0}^2 + x_{4Q0}^2)}$$

$$D_{n2} (7,2) = \frac{x_{4D0}}{T_{d2} (x_{4D0}^2 + x_{4Q0}^2)}$$

$$D_{n2} (10,1) = \left[ \frac{K_p}{T_f} \frac{x_{4D0}}{x_{40}} + K_p \omega_0 \frac{x_{4Q0}}{x_{40}} + K_i \frac{x_{4D0}}{x_{40}} \right]$$

$$D_{n2} (10,2) = \left[ \frac{K_p}{T_f} \frac{x_{4Q0}}{x_{40}} - K_p \omega_0 \frac{x_{4D0}}{x_{40}} + K_i \frac{x_{4Q0}}{x_{40}} \right]$$

$$C_{N1} = \text{zeros} (11, 2)$$

$$C_{N1} (1, 1) = 1/c$$

$$C_{N1} (2, 2) = 1/c$$



$$C_{N1}(8, 1) = \frac{K_{iplltc} * I_{Q0}}{i_D^2 + i_Q^2}$$

$$C_{N1}(9, 1) = \frac{K_{iplltc} * I_{Q0}}{i_D^2 + i_Q^2}$$

$$C_{N1}(8, 2) = \frac{K_{iplltc} * I_{D0}}{i_D^2 + i_Q^2}$$

$$C_{N1}(9, 2) = \frac{K_{iplltc} * I_{D0}}{i_D^2 + i_Q^2}$$

$$C_{N1}(10, 1) = -\frac{K_i * i_{D0}}{\text{sqrt}(i_D^2 + i_Q^2)}$$

$$C_{N1}(10, 2) = -\frac{K_i * i_{Q0}}{\text{sqrt}(i_D^2 + i_Q^2)}$$

$$C_{N2} = \text{zeros}(11, 2)$$

$$C_{N2}(10, 1) = -\frac{K_p * i_{D0}}{\text{sqrt}(i_D^2 + i_Q^2)}$$

$$C_{N2}(10, 2) = -\frac{K_p * i_{Q0}}{\text{sqrt}(i_D^2 + i_Q^2)}$$

$$A_g = \begin{bmatrix} A_e & B_{e3} * C_m \\ B_{m1} * C_{me} & A_m \end{bmatrix}$$

$$B_g = \begin{bmatrix} B_{e1}^t & 0 \end{bmatrix}$$

$$C_g = \begin{bmatrix} C_e & 0 & C_{em} & C_m \end{bmatrix}$$

$$A_t = \begin{bmatrix} A_g + B_g * H * (F * C_g + \frac{X_l}{\omega_b} * C_g * A_g) & B_g * H & \text{zeros}(16,11) \\ B_{n2} * C_g * B_g * (H * (F * C_g + \frac{X_l}{\omega_b} * C_g * A_g)) & A_{n1} + B_{n2} * C_g * B_g * H & D_{n1} \\ C_{n2} * C_g * B_g * H * (F * C_g + \frac{X_l}{\omega_b} * C_g * A_g) & D_{n2} + C_{n2} * C_g * B_g * H & A_{n2} \end{bmatrix}$$

## REFERENCES

---

1. IEEE subsynchronous resonance task force, "First benchmark model for computer simulation of subsynchronous resonance," *IEEE Trans. Power Apparatus and Systems*, vol PAS-96, pp.1565~1572, Sep./Oct.1977.
2. S. G. Jalali, R. A. Hedin, M. Pereira, and K. Sadek, "A stability model for the advanced series compensator (ASC)," *IEEE Trans. Power Del.*, vol. 11, no. 2, pp. 1128–1137, Apr. 1996.
3. C. R. Fuerte-Esquivel, E. Acha, and H. Ambriz-Perez, "A thyristor controlled series compensator model for the power flow solution of practical power networks," *IEEE Trans. Power System.*, vol. 9, no. 15, pp. 58–64, Feb. 2000.
4. IEEE Committee Report, "Terms, definitions and symbols for subsynchronous resonance oscillations," *IEEE T-PAS*, vol. 104, pp.1326-1334, June 1985.
5. D. Jovcic, N. Pahalawaththa, M. Zavahir, and H. Hassan, "SVC dynamic analytical model," *IEEE Trans. Power Del.*, vol. 18, no. 4, Pp.1455–1461, Oct. 2003.
6. R. Mohan Mathur, Rajiv K. Varma, "Thyristor-based facts controllers for electrical transmission systems," New York: Wiley, 2002, pp.315~355.
7. N. G. Hingorani, and L. Gyugyi, *Understanding FACTS*, IEEE press, 1999, pp. 225-239.

9. P. Anderson, B. Agrawal, and J. V. Ness, *Subsynchronous Resonance ZD Power Systems*. New York, N.Y.: IEEE Press, 1990.
10. "Readers Guide to Subsynchronous Resonance," IEEE Committee Report, 1991. IEEE PES Summer Power Meeting, Paper No. 91 SM 350-9 PWRS, San Diego, July, 1991
11. A. Gole, V. K. Sood, and L. Mootosamy, "Validation and analysis of a grid control system using D-Q-Z transformation for static compensator systems," in *Proc. Canada. Conf. Electrical Computer Engineering*, Montreal, QC, Canada, Sep. 1989, pp. 745–748.
12. *PSCAD/EMTDC Users Manual*, 1994. Manitoba HVDC Research Center, Tutorial manual.
13. D. Jovcic and G. N. Pillai, "Discrete system model of a six-pulse SVC," in *Conf. Proc. IASTED Europe's 2003*, Marbella, Spain, Sep. 2003, pp. 318–323.
14. Shem, "Computing the damping of subsynchronous oscillations due to a Thyristor controlled series capacitor," *IEEE Transaction on Power Delivery*, Vol. 11 (2), pp. 1120-1 127, April 1996
15. Modeling of Thyristor Controlled Series Capacitor for SSR Studies," *IEEE Trans. Power Systems*, vol. 11(1), pp. 119-126, February 1996.
16. P. Mattavelli, A. M. Stankovic, and G. C. Verghese, "SSR analysis with dynamic phasor model of thyristor controlled series capacitor," *IEEE Trans. on Power Systems*, Vol. 11, No. 1, February 1996, pp. 119-127.
17. E. Larsen, C. Bowler, B. Damsky, and S. Nilsson, "Benefits of thyristor controlled series compensation," Cigré 37 Session, Paris, 1992.

- 17 Luiz A. S. Pilotto, André Bianco, Willis F. Long, and Abdel-Aty Edris. "Impact of TCSC control methodologies on subsynchronous oscillations", *proceedings of EPRI conference on FACTS, Washington, DC, April 1996.*
- 18 B. K. Perkins, M. R. Iravani, "Dynamic modeling of a TCSC with application to SSR Analysis,"IEEE Trans. Power System, vol. 12, no. 4, NOV. 1997, pp1619-1625
- 19 MATLAB User's Guide. The Math Works, Inc., South Natick, MA.
20. Dragan Jovic, Member, IEEE, and G.N.Pillai,"Analytical modeling of TCSC Dynamics,"IEEE Trans.Power Delivery, vol.20, no.2, APRIL 2005.
21. K.R. Padiyar, Power System Dynamics: Stability and Control, Interline, Bangalore, 1996.